Bridged-T networks
by Nirmal Kumar Dhar Choudhury

A THESIS Submitted to the Graduate Committee in partial fulfillment of the requirements for the degree of Master of Science in Electrical Engineering
Montana State University

Abstract:
Bridged- T networks, though not unknown in the field of radio engineering, have received little attention. Only the resonant conditions of simple symmetrical bridged-T networks have been discussed in literature. This paper deals with bridged-T networks in general and discusses two typical circuits in detail.

Using matrices and Kirchhoff's laws a general mathematical theory of bridged-T networks is developed from consideration of a perfectly general theory applicable to any complex network. From this theory are derived expression for transmission, i.e. the ratio of output voltage to input Voltage, under no-load conditions, and the condition of null transmission of general bridged-! networks. Equations are also derived for transforming these networks (as a matter of fact any complex network) to their equivalent Pi-circuits, These equations are applied to determine the input and output impedances of the network. Two typical bridged-T circuits are then selected for investigation, and the general expressions and equations derived are applied to these particular cases to determine their resonant conditions,, transmission, phase angle, input loading and output loading. These circuits are quite general since both symmetrical and nonsymmetrical circuits are considered.

The circuit characteristics, as determined from the theory are then checked by experimental investigation. Choosing proper circuit elements, transmission and phase-shift characteristics of both circuits are determined for symmetrical and unsymmetrical cases. The experimental results are then compared with the theoretical predictions and are found to be in good agreement.

BRIDGED-T NETWORKS.

by

Nirmal Kumar Dhar Choudhury.

A THESIS

Submitted to the Graduate Committee

in

partial fulfillment of the requirements

for the degree of

Master of Science in Electrical Engineering

at

Montana State College.

Approved:

R. C. Seibel

In Charge of Major Work

R. C. Seibel

Chairman, Examining Committee

J. A. Nelson

Chairman, Graduate Committee

Bozeman, Montana
March, 1948.

Acknowledgement.

This Thesis work was undertaken under the suggestion and guidance of Professor R. C. Seibel of the Electrical Engineering Department, Montana State College, U.S.A. The author expresses his deep appreciation to Professor Seibel whose kind help and proper direction led to the completion of the work.

N.Bhar Chaudhuri

Table of Contents.

....

Abstract.

Bridged-T networks, though not unknown in the field of radio engineering, have received little attention. Only the resonant conditions of simple symmetrical bridged-T networks have been discussed in literature. This paper deals with bridged-T networks in general and discusses two typical circuits in detail.

Using matrices and Kirchhoff's laws, a general mathematical theory of bridged-T networks is developed from consideration of a perfectly general theory applicable to any complex network. From this theory are derived expression for transmission, i.e. the ratio of output voltage to input voltage, under no-load conditions, and the condition of null transmission of general bridged-T networks. Equations are also derived for transforming these networks (as a matter of fact any complex network) to their equivalent Pi-circuits. These equations are applied to determine the input and output impedances of the network. Two typical bridged-T circuits are then selected for investigation, and the general expressions and equations derived are applied to these particular cases to determine their resonant conditions, transmission, phase angle, input loading and output loading. These circuits are quite general since both symmetrical and nonsymmetrical circuits are considered.

The circuit characteristics, as determined from the theory are then checked by experimental investigation. Choosing proper circuit elements, transmission and phase-shift characteristics of both circuits are determined for symmetrical and unsymmetrical cases. The experimental results are then compared with the theoretical predictions and are found to be in good agreement.

Introduction.

Frequency selective networks containing inductance and capacitance have been extensively discussed in literature and widely used in practice. Bridged-T networks of simple types have been in use as wave traps since perfect suppression of a single frequency can be easily obtained, though considerable dissipation is present in the components of the circuit. Rejection characteristics of antiresonant circuits or their equivalents can be improved by the addition of resistances in such a manner as to form a bridged-T network.

In bridged-T networks the component values can be so chosen as to produce perfect null at a desired frequency in either the audio or radio frequency range. Since these circuits are four terminal networks, this property of perfect balance at resonance has been utilized to a limited extent in alternating-current bridge measuring instruments for measuring inductance, capacitance, resistance, quality factor, etc. But in such use of these circuits no attention is paid to their frequency response or phase-shift characteristics; the only requirement being a good balance at the desired frequency.

The other property of bridged-T networks is their selective response over a band of frequencies. The selectivity and phase-shift in these cases can be easily controlled by variation of circuit parameters, this variation being much more flexible than in the case of antiresonant circuits. In view of this advantage bridged-T networks may be used as wave filters having the desired frequency response characteristic over the desired band of frequencies, and also as feed-back circuits in vacuum tube amplifiers.

In operation, bridged-T networks are very simple, the generator and the load being directly connected across the input and output, respectively, without requiring a coupling transformer. Moreover, no balance-to-ground operation is required, the ground terminal being common to both the generator and the load. Hence they require no Wagner earth connection. Their disadvantage is due to insertion loss since they absorb power from the input.

To the author's knowledge very little work of any investigational nature has been done on bridged-T networks. Only the resonant conditions of some simple bridged-T networks have been discussed by Tuttle.[1] In view of the possible wide application of bridged-T networks and in view of some of their inherent merits, a systematic extensive investigation on these circuits was taken up. This paper deals with:

1. A general mathematical theory of bridged-T networks.
2. Transmission and phase-shift characteristics of two typical circuits for different values of circuit Q.
3. Transmission and phase-shift characteristics of two typical circuits having circuit parameters bearing no simple relationship with each other.
4. Dependence of circuit-selectivity and phase-shift on circuit Q and degree of dissymmetry of circuit parameters.
5. Comparison of the experimental results with the theoretical work.

---

1. W. N. Tuttle, BRIDGED-T AND PARALLEL-T CIRCUITS FOR MEASUREMENTS AT RADIO FREQUENCIES, Proc. I.R.E, page 23, January, 1940.

The Mathematical Theory.

The theory of bridged-T networks will be developed from consideration of a very general mathematical theory,[1] which may, with requisite changes, be applied to any complex four terminal network.

Network transmission and resonance:-

The network transmission T will be defined[2] as the vector ratio of the output voltage E_2 to the input voltage E_1, under condition of no load. This condition is closely realized in practice if the load connected across the output terminals has a high impedance. For the no load condition the expression for network transmission, as derived in appendix 1a., is

$$T = \frac{E_2}{E_1} = \frac{Z_1Z_2 + Z_2Z_3 + Z_1Z_3 + Z_3Z_4}{Z_1Z_2 + Z_2Z_3 + Z_1Z_3 + Z_3Z_4 + Z_1Z_4} \quad \ldots\ldots\ldots \; 4.$$

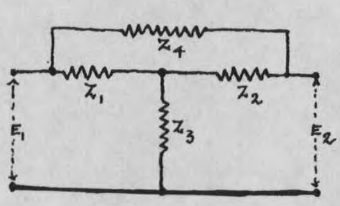

Fig. 1.

---

1. M. B. Reed, GENERAL FORMULAS FOR T AND Π-NETWORKS EQUIVALENTS, Proc. I.R.E., pp 897, December, 1945.

2. L. Stanton, THEORY AND APPLICATION OF PARALLEL-T RESISTANCE-CAPACITANCE FREQUENCY SELECTIVE NETWORKS, Proc. I.R.E., pp 447, July, 1946.

It may be noted that the network transmission T will be zero when the numerator of the expression for T is zero. Under this condition the whole circuit appears as an infinite impedance to the source. This condition is called resonance, since the behaviour is similar to the resonance of a parallel L-C circuit. Hence the condition of null transmission or resonance of the general bridged-T network is given by the equation

$$Z_1Z_2 + Z_2Z_3 + Z_1Z_3 + Z_3Z_4 = 0 \quad \ldots\ldots\ldots\ldots\ldots\ldots\ldots\ldots 5.$$

where the disposition of the component impedances Z_1, etc. is shown in Fig. 1.

Equivalent Pi-circuit.

In order to facilitate the study of some of the special characteristics of bridged-T networks, the given circuit is transformed to its equivalent Pi-circuit shown by Fig. 2. The relationship between the component impedances of the equivalent Pi-circuit and those of the original circuit, as derived in appendix 1b, is given by the following equations.

$$Z_A = \frac{Z_1Z_2 + Z_2Z_3 + Z_1Z_3}{Z_2} \quad \ldots\ldots\ldots 9a.$$

$$Z_B = \frac{Z_1Z_2 + Z_2Z_3 + Z_1Z_3}{Z_1} \quad \ldots\ldots\ldots 9b.$$

$$Z_C = \frac{Z_4(Z_1Z_2 + Z_2Z_3 - Z_1Z_3)}{Z_1Z_2 + Z_2Z_3 + Z_1Z_3 + Z_3Z_4} \quad \ldots 9c.$$

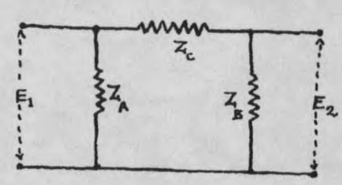

Fig. 2.

From the equivalent Pi-circuit it may also be found, as given in appendix 1c, that

$$T = \frac{E_2}{E_1} = \frac{1}{1 + Z_C/Z_B} \qquad \ldots\ldots\ldots\ldots\ldots\ldots 11.$$

If in this equation the values of Z_B and Z_C are substituted from Eq. 9, the expression for T is identical with that of Eq. 4, as it should be. The Eq. 11 clearly indicates that transmission T is zero when the ratio Z_C/Z_B is infinite. Since Z_B can never be zero owing to its finite component impedances, Z_C/Z_B is infinite only when the denominator of Z_C is zero, that is

$$Z_1Z_2 + Z_2Z_3 + Z_1Z_3 + Z_3Z_4 = 0, \qquad \ldots\ldots\ldots\ldots\ldots\ldots 5.$$

which is the same condition for null transmission as derived earlier.

Input and output loading.

Bridged-T networks place a load across the source as well as the detector. These loads can be determined from the equivalent Pi-circuit. Both the input and output loading vary with frequency in a complicated manner and are extremely difficult to determine theoretically. However, it is relatively easy to find, theoretically, the loading at resonance, since the impedance Z_C is then infinite. The input and output impedances of the circuit are Z_A and Z_B, respectively, where Z_A and Z_B are given by Eq. 9. As the frequency deviates from resonance, Z_C is no longer infinite and hence both the input and output impedances vary in a manner which could be determined experimentally.

Thus,

Input impedance at resonance $= Z_A$ ....12.

Output impedance at resonance $= Z_B$ ....13.

These are the impedances at resonance which the bridged-T circuit puts in parallel with the generator and the detector or load.

Bridged-T Network Type 1.

The first bridged-T network that was investigated is shown in Fig. 3. In this circuit the bridging arm consists of an inductance in series with a resistance, which in some cases may be the coil resistance alone.

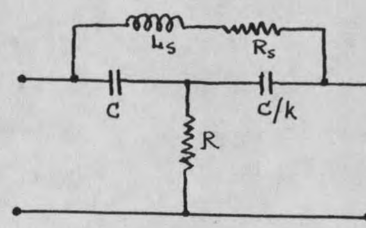

Fig. 3.

The arbitrary number k gives the degree of dissymmetry of the circuit. If k = 1, the circuit is symmetrical.[1] The two equations that the circuit must satisfy for null transmission, or resonance, are developed in appendix 2a. They are

$$R.R_s = k/(\omega C)^2 \qquad \text{.................15.}$$

and

$$\omega L_s = \frac{1 + k}{\omega C} \; . \qquad \text{.................16.}$$

For a symmetrical circuit the conditions reduce to

$$R.R_s = 1/(\omega C)^2$$

$$\omega L_s = 2/\omega C,$$

which are exactly Tuttle's conditions of resonance. From Eq. 16, it may

1. W.N.Tuttle, BRIDGED-T AND PARALLEL-T CIRCUITS FOR MEASUREMENT AT RADIO FREQUENCIES, Proc. I.R.E., pp 23, January, 1940.

F.E.Terman, RADIO ENGINEER'S HANDBOOK, First edition, pp 918.

be observed that the resonant frequency is the frequency at which the two capacities in series are in parallel resonance with L_s. Thus at resonance the circuit behaves as if an antiresonant circuit were placed in series with the line. Hence Eq. 16 is the frequency determining equation which fixes the resonant frequency of the circuit. If Eq. 15 is satisfied the transmission will be zero at resonance; otherwise it will simply pass through a minimum at the resonant frequency.

Circuit transmission.

The expression for circuit transmission under no load condition, as derived in appendix 2b, is

$$T = \frac{1}{1 + j\,\frac{\gamma}{1-\gamma^2}\cdot\frac{1+k}{k}\cdot\frac{1}{Q_o}} \qquad \ldots\ldots\ldots\ldots 17.$$

Hence the magnitude of T is

$$|T| = \frac{1}{\sqrt{\left[1 + \left(\frac{\gamma}{1-\gamma^2}\cdot\frac{1+k}{k}\cdot\frac{1}{Q_o}\right)^2\right]}} \qquad \ldots\ldots\ldots\ldots 18.$$

and the phase angle θ of T, i.e., the angle by which E_x leads or lags E_1 is

$$\theta = -\tan^{-1}\frac{\gamma}{1-\gamma^2}\cdot\frac{1+k}{k}\cdot\frac{1}{Q_o}, \qquad \ldots\ldots\ldots\ldots 19.$$

where

$$\gamma = \frac{f}{f_o} = \frac{\omega}{\omega_o} = \frac{\text{actual frequency}}{\text{resonant frequency}}$$

and $Q_o = \omega L_s/R_s$ = quality factor of the coil including the series resistance, if any.

These simple expressions for T and Q indicate that at resonance, when $\gamma = 1$, the transmission is zero and phase angle is $\pm 90^\circ$. For high circuit selectivity off-resonance transmission must be high, which occurs when both Q_o and k are large. It may be noted here that for a given value of C and of f_o higher values of k will automatically necessitate higher values of L_s and consequently higher Q_o. The effect is therefore cumulative towards higher selectivity. Moreover, larger values of Q_o and k will produce less phase-shift at frequencies off resonance. Hence maximum transmission at a given frequency will also correspond to minimum phase-shift. The phase-shift characteristic is such that the phase angle decreases on both sides of the resonant frequency.

There are some limitations against the use of higher values of Q_o and k. One limitation against the use of high values of k is that it makes the capacity C/k of Fig. 3 small for a given value of C. Under such circumstances the effect of stray capacity will be noticeable. The effect of stray capacity is negligible only when it is small compared with the effective capacity C/(1 + k) of the circuit.

Another limitation is that higher values of k and Q_o will increase the input and output loading as is evident from Eqs. 23 and 24. Higher input loading means shunting the generator by the network. Hence for smaller input loading both k and Q_o should be small. For low output loading Q_o should not be very large, but k should be large.

Input and output loading.

The expression for input impedance at resonance, as derived in appendix 2c, is

$$|Z_{io}| = \frac{1+k}{k} \cdot R\sqrt{1+1/Q_o^2} \quad \ldots\ldots\ldots\ldots 23.$$

For small loading of the source $|Z_{io}|$ must be large. Hence R must essentially be large. Moreover, for low loading both k and Q_o should be small as has already been stated. Thus the values of k and Q_o should be so selected as to make a compromise between high selectivity and low input-loading.

The output impedance of the circuit at resonance, as found in appendix 2c, is

$$|(Z_{out})_o| = (1+k)\, R\sqrt{1+1/Q_o^2} \quad \ldots\ldots\ldots\ldots 24.$$

For low output loading also R must be large. Small values of Q_o and large values of k are desirable.

It may therefore be mentioned that the values of k and Q_o should be carefully chosen so as to make a reasonable compromise between network selectivity and input and output loading.

Effect of stray capacity.

It should be noted that the capacity of the junction point O, Fig. 4, with respect to ground is not without effect, since the impedance level of the point O at resonance is high. The capacity of the points A and B with respect to ground are across the

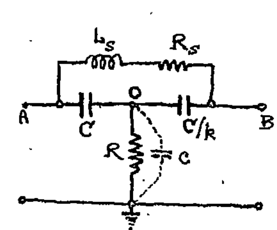

Fig. 4

source and the detector, respectively, and hence do not affect the circuit behaviour. If the effect of c is considered, the conditions of resonance are altered as shown in appendix 4a. They are

$$R.R_S = k/(\omega C)^2 \quad \ldots\ldots\ldots\ldots 15.$$

and

$$\omega L_S = \frac{1 + k}{\omega C} \left[1 + \frac{k c}{(1 + k)C} \right]. \quad \ldots\ldots\ldots\ldots 40.$$

These equations show that while the first condition remains unaltered the resonant frequency given by the second condition is slightly increased by the term kc/(1+k)C. In order that the effect of c will not disturb the circuit behaviour, c must be very small compared with C. The effective capacity in presence of c is given by

$$C' = \frac{C^2}{(1+k)\ C + kc}, \quad \ldots\ldots\ldots\ldots 41.$$

where kc is the correction term, and this should be small compared with (1+k)C.

Bridged-T Network Type 2.

The second bridged-T circuit that was placed under investigation is shown in Fig. 5. The bridging arm in this circuit consists of a simple resistance, while the shunting arm consists of an inductance in parallel with a resistance. As before, the magnitude of k represents the degree of departure from a symmetrical network. The two equations that the circuit must satisfy for null transmission, or resonance, are developed in appendix 3a. They are

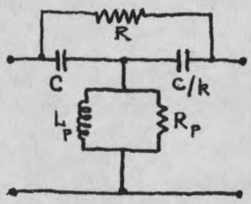

Fig. 5

$$R.R_p = k/(\omega C)^2 \qquad \ldots\ldots\ldots\ldots\ldots\ldots 28.$$

and

$$\omega L_p = \frac{k}{1+k} \cdot \frac{1}{\omega C} \cdot \qquad \ldots\ldots\ldots\ldots\ldots\ldots 29.$$

For a symmetrical circuit $k = 1$, and the equations reduce to

$$R.R_p = 1/(\omega C)^2$$

$$\omega L_p = 1/2\omega C,$$

which are exactly Tuttle's conditions of resonance. It may be observed from Eq. 29 that the resonant frequency is the frequency at which the two capacities C and C/k in parallel produce resonance with L_p. At resonance the whole circuit behaves as if a compensated series resonant circuit was placed across the line shunting the source. Also, Eq. 29 is the frequency determining equation which fixes the resonant frequency of the circuit. If Eq. 28 is satisfied the transmission will be zero at resonance; otherwise it will merely pass through a minimum at the resonant frequency.

Circuit transmission.

The expression for circuit transmission under no load condition, as derived in appendix 3b, is

$$T = \frac{1}{1 + j\frac{\gamma}{1-\gamma^2} \cdot \frac{1+k}{k} \cdot Q_o} \quad \text{..................30.}$$

Hence the magnitude of T is

$$|T| = \frac{1}{\sqrt{\left[1 + \left(\frac{\gamma}{1-\gamma^2} \cdot \frac{1+k}{k} \cdot Q_o\right)^2\right]}} \quad \text{..................31.}$$

And the phase angle of T, i.e., the angle by which E_2 leads or lags E_1 is

$$\theta = -\tan^{-1} \frac{\gamma}{1-\gamma^2} \cdot \frac{1+k}{k} \cdot Q_o \quad \text{..........................32.}$$

where γ represents the fractional detuning from resonance, i.e., the ratio of the actual frequency to the resonant frequency. Q_o represents a ratio of the reactance of the coil at the resonant frequency to the resistance R_p, i.e., $Q_o = \omega_o L_p / R_p$.

These simple expressions for T and θ indicate that at resonance, when $\gamma = 1$, the circuit transmission is zero and the phase-angle is $\pm 90^\circ$. For high selectivity of the circuit, off-resonance transmission must be high which occurs when Q_o is small and k is large. Moreover, smaller values of Q_o and greater values of k will produce less phase shift at frequencies off resonance. Hence maximum transmission at a given frequency will also correspond to minimum phase shift. The phase shift characteristic is such that the phase angle decreases on both sides of the resonant frequency.

There are limitations against making Q_o too small and k too large. If Q_o is very small there is heavy input loading. Under the limits of proper input loading, the best value of Q_o would range from 0.2 to 1. If k is made large the effect of stray capacity will affect the circuit characteristics. Hence in designing the circuit a compromise should be made between high selectivity and low loading.

Input and output loading.

The expression for input impedance at resonance, as derived in appendix 3c, is

$$|Z_{io}| = \frac{1 + k}{k} \cdot \frac{\omega_o L_p}{\sqrt{[(1 + 1/Q_o)^2]}} \qquad \ldots\ldots\ldots 36.$$

For small loading of the source the input impedance must be large. This requires that $\omega_o L_p$ be large and also R_p be equally large. For a good compromise between high selectivity and low loading a desirable value of Q_o is 1, whence

$$|Z_{io}| = \frac{1 + k}{k} \cdot \frac{\omega_o L_p}{\sqrt{2}} .$$

The output impedance of the circuit at resonance, as found in appendix 3c, is

$$|(Z_{out})_o| = (1+k)\ \omega_o L_p/\sqrt{[1 + 1/Q_o^2]}. \qquad \ldots\ldots\ldots 37.$$

For low output loading $\omega_o L_p$ and R_p should be large.

Effect of stray capacity.

As with the previous circuit, the capacity between the junction point O, Fig. 6, and the ground has a modifying effect on the circuit behaviour. But since in this circuit the impedance level at resonance is very low, the effect of c is also very small. As before, the capacity of the points A and B with respect to ground are across the source and the detector, respectively, and hence do not affect the circuit behaviour.

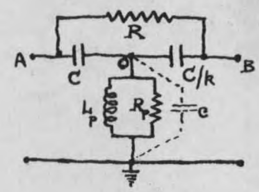

Fig. 6.

If the effect of this stray capacity c is taken into account, it is shown in appendix 4b that the resonant conditions are

$$R.R_p = k/(\omega C)^2 \qquad \ldots\ldots\ldots\ldots\ldots\ldots 28.$$

and

$$\omega L_p = \frac{1}{\omega[(1+k)C/k + c]}. \qquad \ldots\ldots\ldots\ldots\ldots\ldots 44.$$

These show that while the first condition remains unaltered, the resonant frequency given by the second condition is slightly decreased due to the term c. In order that the effect of c would be negligible, C must always be large in comparison with c. The effective capacity including c is given by

$$C' = (1+k)C/k + c. \qquad \ldots\ldots\ldots\ldots\ldots\ldots 45.$$

This equation indicates that c is effectively in parallel with the two capacitors C and C/k acting in parallel.

Experimental Setup.

Experimental investigations were undertaken on the two typical bridged-T circuits under discussion. The object of these experimental studies was to determine the transmission and phase-shift characteristics for different values of the circuit parameters.

Experimental setups are shown by the block diagrams below. Fig. 7 shows the arrangement used for measurement of circuit transmission, whereas Fig. 8 shows the arrangement used for measurement of phase angles.

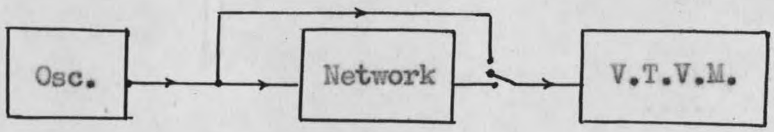

Fig. 7.

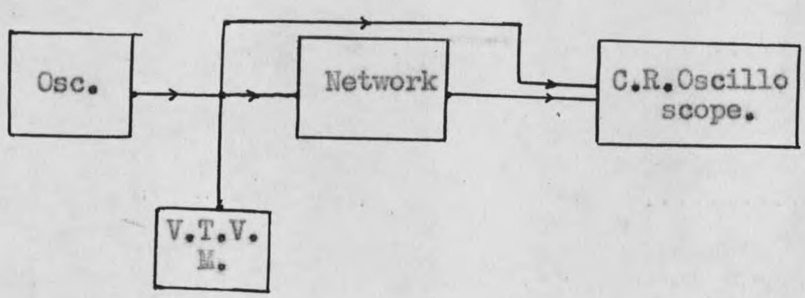

Fig. 8.

Noninductive resistors of the composition type were used in the circuits. Both mica and paper dielectric capacitors of high quality were used, hence the condensers were essentially loss-free. The circuit elements were always measured in an impedance bridge to check their marked values. The output impedances of the audio oscillators used were specified as 500 ohms and they were practically free from harmonics. The R.F oscillator had different output impedances at its different ranges, and contained appreciable harmonics. The input impedance of the detector, a vacuum tube voltmeter, was above several meghohms even at the highest radio frequencies used, so that no load conditions were truly fulfilled.

Circuit transmissions were measured in the usual way. The phase angles were measured from the dimensions of the ellipses formed on the oscilloscope screen. If b = intercept along the X-axis from the center of the ellipse, a = maximum horizontal distance of projection of the ellipse along the X-axis,

The phase angle[1] is given as $\theta = \sin^{-1} b/a$.

1. E.H. Schulz and L.T. Anderson, EXPERIMENTS IN ELECTRONICS AND COMMUNICATION ENGINEERING, pp 165.

Experiment on circuit 1.

Experiments on this circuit, Fig. 3, were conducted to determine the transmission and phase shift characteristics for different values of coil Q and for different values of k, both in the high and low frequency region.

1. Low frequency region:- Between 5 kc and 20 kc.

The circuit designed for these measurements was symmetrical, the values of R and R_s being so selected as to make a compromise between circuit selectivity and circuit loading. The series resistance R_s and the shunting resistance R had different values for each value of Q_o used. For each set of data R_s was first selected to give the desired Q_o and the value of R was finally adjusted during experiment until the circuit transmission was exactly nill at resonance. At this point the resonant condition as given by Eq. 15 was satisfied.

The inductance of the coil at 1000 cycles and the resistance R_s, which includes the coil resistance, were measured by an impedance bridge. The Q of the coil was measured by the same bridge at 1000 cycles and its value at the resonant frequency was computed, assuming Q to be directly proportional to frequency within this small range of frequency.

Table 1.

Circuit 1.

L_s = 5.25 mh. C_s = C/k = 0.05 μF. R_s = 62 ohms.

f_o = 13.85 kc. k = 1. R = 870 ohms.

Q_o = 0.5 x 13.85 = 6.925.

		Transmission			Phase angle E_{in} = 10 volts.			
γ	f kc	E_{in}	E_{out}	Tx100.	2b	2a	b/a	Θ
0.6	8.32	10 v	9.75	97.5	9.65	35.7	0.27	15.7°
0.7	9.70	"	9.45	94.5	13.3	34.4	0.387	22.8°
0.8	10.8	"	8.8	88.0	17.3	31.8	0.539	32.5°
0.85	11.76	"	7.5	75.0	19.5	27.4	0.713	45.5°
0.9	12.46	"	5.8	58.0	18.2	21.5	0.846	57.8°
0.93	12.89	"	4.4	44.0	15.6	16.9	0.923	67.5°
0.96	13.29	"	2.75	27.5	9.6	10.0	0.96	77.7°
0.98	13.56	"	1.35	13.5	..	..	..	..
1.0	13.85	"	0	0	..	..	..	±90°
1.02	14.12	"	1.3	13.0	..	..	..	..
1.04	14.4	"	2.4	24.0	9.0	9.3	0.968	75.5°
1.07	14.82	"	3.7	37.0	14.0	15.0	0.947	71.2°
1.1	15.22	"	5.05	50.5	18.3	20.8	0.88	61.7°
1.15	15.91	"	6.4	64.0	18.2	23.3	0.782	51.5°
1.2	16.6	"	7.45	74.5	18.3	27.2	0.673	42.3°
1.3	18.0	"	8.45	84.5	16.2	30.5	0.532	32.1°
1.4	19.4	"	9.0	90.0	13.5	30.9	0.437	25.9°

Table II.

Circuit 1.

L_s = 5.25 mh.   C = C/k = 0.05 μF. R_s = 33.7 ohms.

f_o = 13.85 kc.   k = 1.   R = 1500 ohms.

Q_o = 0.94 x 13.85 = 13.0

		Transmission			phase angle			
γ	f kc	E_{in}	E_{out}	Tx100	2b	2a	b/a	θ
0.7	9.70	10v	9.8 v	98.0	6.0	33.3	0.18	10.4°
0.8	10.8	"	9.45	94.5	10.0	31.6	31.6	18.5°
0.85	11.76	"	8.8	88.0	13.85	29.5	0.47	28.°
0.9	12.46	"	7.6	76.0	16.6	25.4	0.654	40.7°
0.93	12.89	"	6.25	62.5	16.3	21.1	0.773	50.6°
0.96	13.29	"	4.3	43.0	12.7	13.9	0.915	66.2°
0.98	13.56	"	2.3	23.0	..	..	..	..
1.0	13.85	"	0	0	..	..	..	±90°
1.02	14.12	"	2.4	24.	..	..	..	..
1.07	14.82	"	5.7	57.0	14.5	17.9	0.81	54.1°
1.1	15.22	"	7.2	72.0	16.0	24.4	0.656	41.°
1.15	15.91	"	8.15	81.5	15.3	26.4	0.58	35.4°
1.2	16.6	"	8.8	88.0	12.0	28.9	0.415	24.5°
1.3	18.0	"	9.4	94.0	9.4	30.3	0.31	18.°
1.4	19.4	"	9.6	96.0	7.0	31.5	0.222	12.8°

Table III.

Circuit 1.

L_s = 5.25 mh. C = C/k = 0.05 μF. R_s = 9.3 ohms.

f_o = 13.85 kc. k = 1 R = 5,500 ohms.

$Q_o = 3.5 \times 13.85 = 48.1.$

		Transmission			Phase angle			
γ	f kc	E_{in}	E_{out}	Tx100	2b	2a	b/a	θ
0.7	9.70	10v	10v	100.	3.5	38.8	0.09	5.2°
0.8	10.8	"	9.9	99.0	5.8	37.0	0.157	9°
0.85	11.76	"	9.7	97.0	9.0	36.7	0.245	14.2°
0.9	12.46	"	9.1	91.0	13.5	35.1	0.385	22.7°
0.93	12.89	"	8.4	84.0	16.7	33.1	0.505	30.3°
0.96	13.29	"	7.0	70.0	19.5	26.3	0.742	47.9°
0.98	13.56	"	4.6	46.0	17.9	20.2	0.887	62.5°
1.0	13.85	"	0	0	..	..	..	±90°
1.02	14.12	"	3.0	30.0	13.7	15.1	0.908	65.2°
1.04	14.4	"	6.25	62.5	19.4	26.7	0.727	46.7°
1.07	14.82	"	8.0	80.0	17.1	30.1	0.569	34.7°
1.1	15.22	"	8.93	89.3	14.5	33.0	0.439	26.1°
1.15	15.91	"	9.4	94.4	11.7	34.4	0.34	19.8°
1.2	16.6	"	9.7	97.0	9.0	35.0	0.257	14.9°
1.3	18.0	"	9.82	98.2	5.3	37.0	0.143	8.2°
1.4	19.4	"	9.9	99.0	3.0	38.0	0.079	4.5°

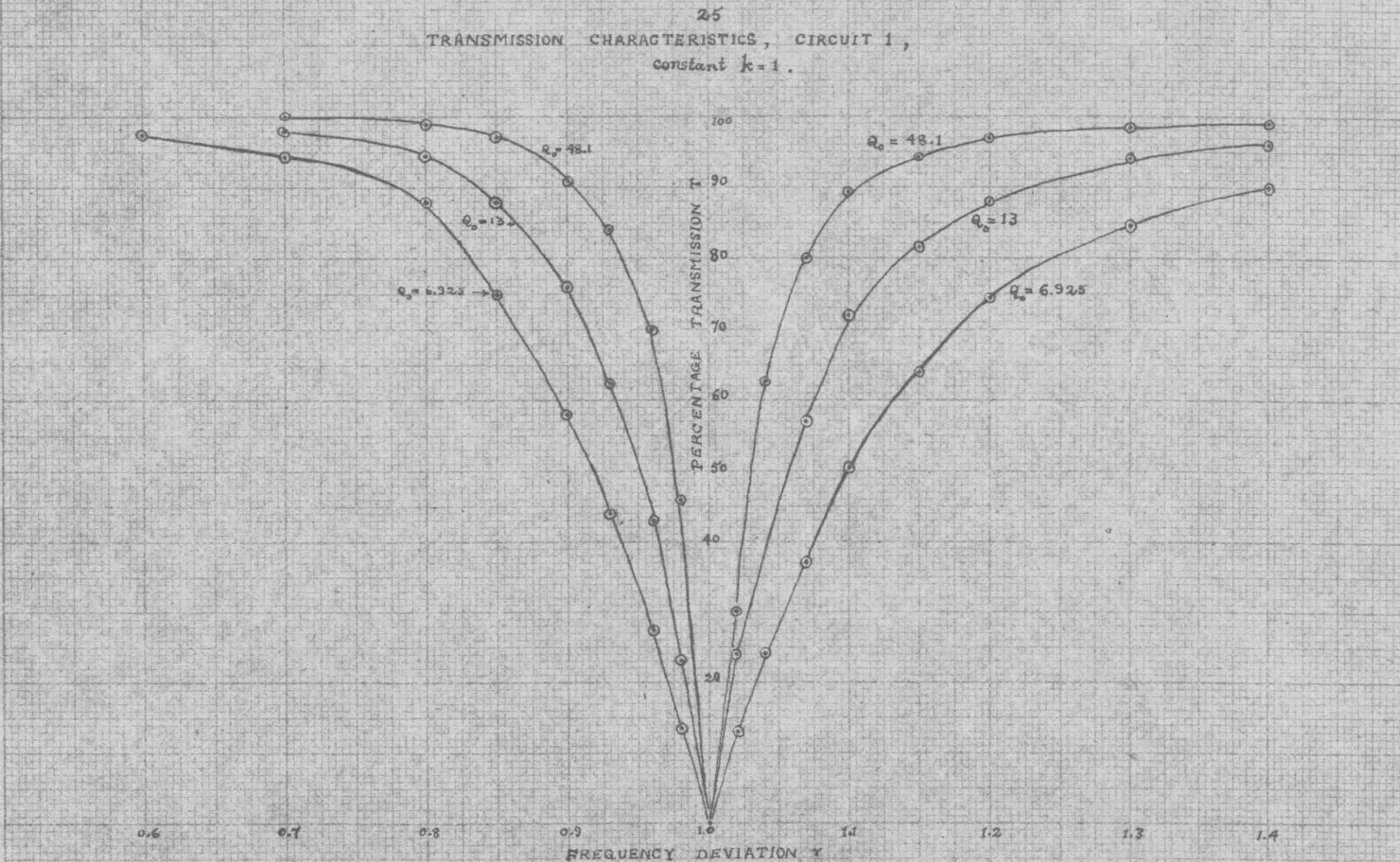
TRANSMISSION CHARACTERISTICS, CIRCUIT 1,
constant k = 1.
PERCENTAGE TRANSMISSION T
FREQUENCY DEVIATION Y
Q0 = 48.1
Q0 = 13
Q0 = 6.925
100
90
80
70
60
50
40
20
0.6
0.7
0.8
0.9
1.0
1.1
1.2
1.3
1.4

FIG. 9.

PHASE - SHIFT CHARACTERISTICS, CIRCUIT 1,

CONSTANT k=1.

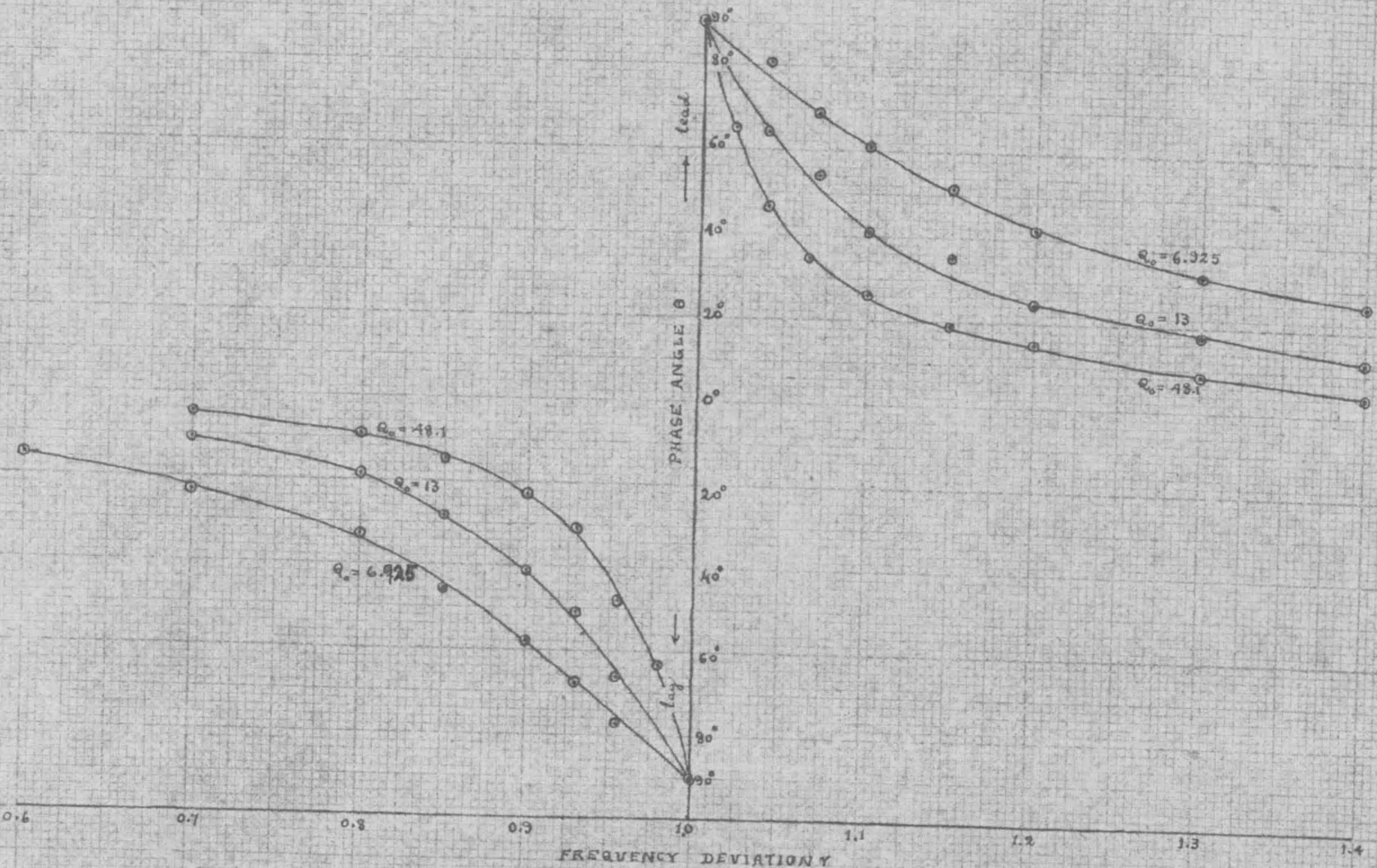

Fig. 10.

2. High frequency region:— Between 90 kc and 200 kc.

In these measurements circuits were designed for determination of transmission characteristics for different values of Q_o and k. Suitable values of Q_o having a wide range were chosen. The experimental procedure was exactly the same as before with the exception that the inductance of the coil and its quality factor were measured in a different way. The coil and a variable dacade capacitor were connected in parallel to form a parallel resonant circuit. A pentode amplifier using a type 6SJ7 tube in a standard circuit with the resonant circuit as its load impedance was built up. Measurements were taken at a frequency very close to the resonant frequency of the bridged-T circuits under experiment. From a knowledge of the resonant frequency of the pentode amplifier tank circuit and the gain of the amplifier, the coil inductance and Q_o were computed as follows:—

$$L_s = 1/(2\pi f_o)^2 C,$$

where C is the tuning capacity.

$$\text{Amplifier gain}^1 = g_m Q/2\pi f_o C,$$

where $g_m = 1600$, is the mutual conductance of the tube (measured value). It may be noted here that the resistance R_s included the coil resistance plus the series resistance if any. The Q at any other frequency and with other values of the resistance R_s was computed by noting that Q is directly proportional to the frequency and inversely proportional to the resistance within this small range of frequency variation.

---

1. F.E.Terman, RADIO ENGINEER'S HANDBOOK, First Edition, pp 435.

The experimental data is given in tables IV through X, the correspon-ding plots for different Q are shown in Fig. 11 and those for k in Fig. 12.

Table IV.

Circuit 1.

L_S = 618 μh. C = C/k = 0.005 μF. R_S = 4.3 ohms.

f_o = 129.5 kc. k = 1. R = 10,000 " .

Measured amplification at 143 kc = 104. Hence, Q_o = 107.

γ	f kc	E_{in}	E_{out}	Tx100.
0.7	90.5	0.4 v	0.4 v	100
0.8	103.5	"	"	100
0.85	110.0	"	0.398	99.5
0.9	116.5	0.5	0.495	99.0
0.93	120.5	"	0.49	98.0
0.95	123.0	"	0.49	98.0
0.97	125.5	"	0.48	96.0
0.98	127.0	"	0.425	85.0
0.99	128.2	"	0.32	64.0
1.0	129.5	"	0.08	16.0
1.01	131.0	"	0.26	52.0
1.02	132.2	"	0.38	76.0
1.03	133.5	"	0.435	87.0
1.05	136.0	"	0.48	96.0
1.07	138.5	"	0.5	100
1.1	142.5	"	0.5	100

Table V.

Circuit 1.

$L_s = 618\ \mu h.$ $C = C/k = 0.005\ \mu F.$ $R_s = 9.3$ ohms.

$f_o = 129.5$ kc. $k = 1.$

$Q_o = 107 \times 4.3/9.3 = 49.5.$

γ	f kc	E_{in}	E_{out}	Tx100.
0.7	90.5	0.4 v	0.4 v	100
0.8	103.5	0.5	0.49	98.0
0.85	110.0	"	0.49	98.0
0.9	116.5	"	0.48	96.0
0.93	120.5	"	0.48	96.0
0.95	123.0	"	0.47	94.0
0.97	125.5	"	0.42	84.0
0.98	127.0	"	0.34	68.0
0.99	128.2	"	0.2	40.0
1.0	129.5	"	0.08	16.0
1.01	131.0	"	0.2	40.0
1.02	132.2	"	0.32	64.0
1.03	133.5	"	0.38	76.0
1.05	136.0	"	0.46	92.0
1.07	138.5	"	0.49	98.0
1.1	142.5	"	0.5	100

Table VI.

Circuit I.

$L_s = 618\ \mu h.$ $C = C/_k = 0.005\ \mu F.$ $R_s = 15.3$ ohms.

$f_o = 129.5$ kc. $k = 1.$

$Q_o = 107 \times 4.3/15.3 = 30.$

γ	f kc	E_{in}	E_{out}	Tx100.
0.7	90.5	0.4 v	0.4 v	100
0.8	103.5	"	0.39	97.5
0.85	110.0	"	0.385	96.2
0.9	116.5	0.5	0.47	94.0
0.92	119.0	"	0.46	92.0
0.94	121.5	"	0.455	91.0
0.96	124.5	"	0.395	79.0
0.98	127.0	"	0.26	52.0
0.99	128.2	"	0.155	31.0
1.0	129.5	"	0.08	16.0
1.01	131.0	"	0.16	32.0
1.02	132.2	"	0.24	48.0
1.03	133.5	"	0.33	66.0
1.05	136.0	"	0.42	84.0
1.07	138.5	"	0.46	92.0
1.1	142.5	"	0.5	100

Table VII.

Circuit 1.

$L_s = 618\ \mu h.$ $C = C/k = 0.005\ \mu F.$ $R_s = 26$ Ohms.

$f_o = 129.5$ kcs. $k = 1.$

$$Q_o = 107 \times 4.3/26 = 17.8.$$

γ	f kc	E_{in}	E_{out}	Tx100
0.7	90.5	0.4 v	0.4 v	100
0.8	103.5	"	0.39	97.5
0.85	110.0	0.5	0.47	94.0
0.9	116.5	"	0.46	92.0
0.93	120.5	"	0.43	86.0
0.95	123.0	"	0.38	76.0
0.97	125.5	"	0.28	56.0
0.98	127.0	"	0.18	36.0
0.99	128.2	"	0.14	28.0
1.0	129.5	"	0.09	18.0
1.01	131.0	"	0.13	26.0
1.02	132.2	"	0.18	36.0
1.03	133.5	"	0.24	48.0
1.05	136.0	"	0.335	67.0
1.07	138.5	"	0.395	79.0
1.1	142.5	"	0.45	90.0

Table VIII.

Circuit 1.

L_s = 618 μh. C = 0.02 μF. C/k = 0.005 μF.

k = 4. f_o = 102.6 kc. R_s = 4.3 ohms.

Q_o = 90.

γ	f kc	E_{in}	E_{out}	Tx100
0.9	92.5	0.4 v	0.4 v	100
0.93	95.5	"	0.4	100
0.95	97.7	"	0.4	100
0.97	99.7	"	0.39	97.2
0.98	100.5	"	0.38	95.0
0.99	101.6	"	0.34	85.0
1.0	102.6	"	0.085	21.0
1.01	103.8	"	0.32	80.0
1.02	104.8	"	0.37	92.5
1.03	105.8	"	0.39	97.2
1.04	106.9	"	0.398	99.5
1.05	107.95	"	0.4	100

Table IX.

Circuit 1.

L_s = 618μh.

R_s = 4.3 ohms.

f_o = 112.7 kc.

C = 0.01μF.

C/k = 0.005μF.

k = 2.

Q_o = 92.2.

γ	f kc	E_{in}	E_{out}	Tx100
0.9	101.5	0.4 v	0.4 v	100
0.93	104.9	"	0.4	100
0.95	107.0	"	0.4	100
0.97	109.3	"	0.395	99.0
0.98	110.4	"	0.38	95.0
0.99	111.5	"	0.31	77.5
1.0	112.7	"	0.08	20.0
1.01	113.9	0.5	0.355	71.0
1.02	115.0	"	0.44	88.0
1.03	116.1	"	0.475	95.0
1.05	118.4	"	0.5	100
1.07	120.5	"	0.5	100
1.1	124.0	"	0.5	100

Table X.

Circuit 1.

$L_S = 618 \mu h.$

$R_S = 4.3$ ohms.

$f_o = 112.7$ kc.

$C = 0.005 \mu F.$

$C/k = 0.01 \mu F.$

$k = 0.5.$

$Q_o = 92.2.$

γ	f kc	E_{in}	E_{out}	Tx100
0.8	90.0	0.4 v	0.4 v	100
0.9	101.5	"	0.395	99.2
0.93	104.9	"	0.39	97.5
0.95	107.0	"	0.38	95.0
0.97	109.3	0.5	0.415	83.0
0.98	110.4	"	0.36	72.0
0.99	111.5	"	0.24	48.0
1.0	112.7	"	0.07	14.0
1.01	113.9	"	0.22	44.0
1.02	115.0	"	0.34	68.0
1.03	116.1	"	0.405	81.0
1.05	118.4	"	0.48	96.0
1.07	120.5	"	0.5	100
1.1	124.0	"	0.5	100

TRANSMISSION CHARACTERISTICS, CIRCUIT 1, CONSTANT k = 1.

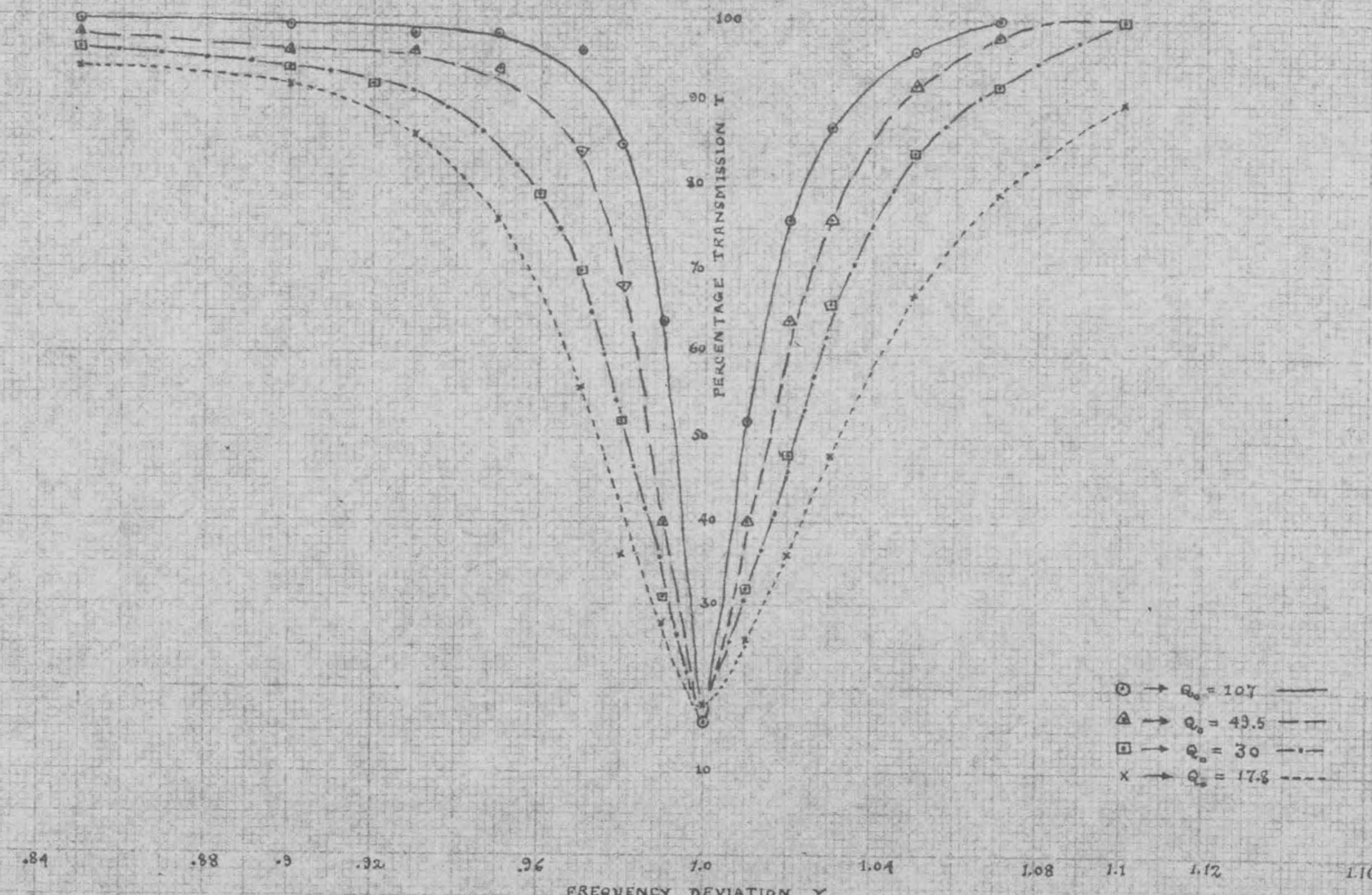

Fig. 11.

TRANSMISSION CHARACTERISTICS, CIRCUIT 1.

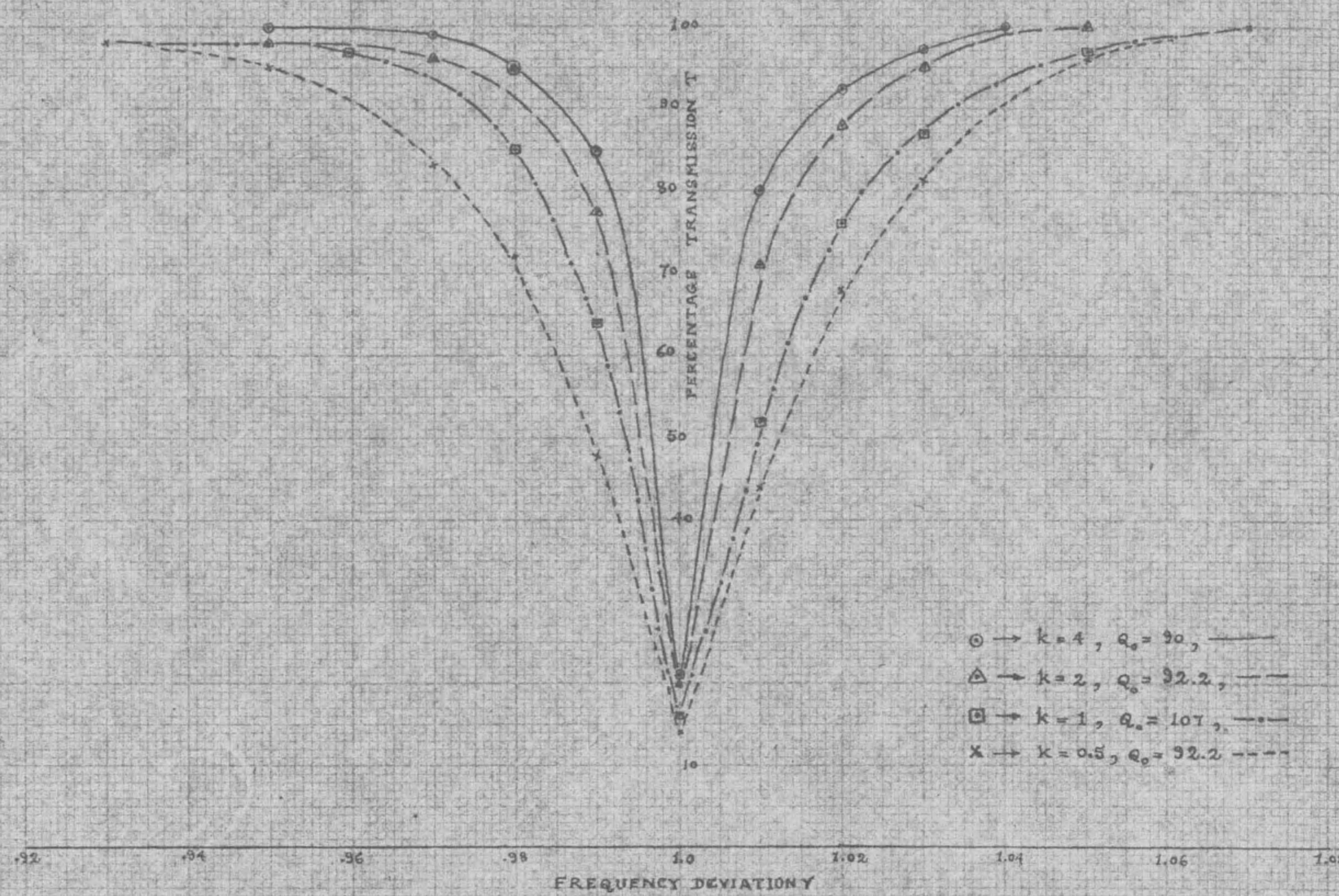

Fig. 12.

Discussion.

At this stage a comparison of the experimental results will be made with the theoretical derivations. Resonant frequencies of the circuits used were calculated from Eq. 16, and the values of R that correspond to null transmission at resonance were evaluated from Eq. 15. The computed and experimental values are given below for comparison. The experimental values of R shown in table XII were measured by use of an ohmmeter contained in a commercial multimeter. Hence the measured values of R were not determined with a high degree of accuracy.

Table XI.

Comparison of resonant frequencies.

Reference to table	Calculated values	Experimental values
I to III	13.89 kcs.	13.85 kcs.
IV to VII	128. "	129.5 "
VIII	101.3 "	102.6 "
IX to X	111.2 "	112.7 " .

Table XII.

Comparison of the values of R.

Reference to table	Calculated values	Experimental values
I	852.5 ohms	870. ohms
II	1,568 "	1,500 "
III	5,683 "	5,500 "
IV	14,500 "	10,000 " .

Comparison of the experimental and calculated values of the resonant frequency and of the shunting resistance R reveals good agreement within the limits of experimental accuracy, thus supporting equations 15 and 16.

It may be mentioned that capacities smaller than 0.003μF were not used in the circuits because the effect of c, the stray capacity at the junction point, was then noticeable in altering the circuit performance.

The transmission and phase-shift characteristics of the circuit can be calculated from Eqs. 18 and 19 respectively. Such calculations and results are shown in tables XIII and XIV.

The experimental transmission and phase-shift characteristics are compared with the theoretical curves in Fig. 13. It is evident that the theoretical and experimental curves for $Q_o = 13$ differ only slightly and in only certain regions, the maximum deviation not exceeding 7 percent. This deviation is due to error involved in accurate measurement of Q_o. The curves for $Q_o = 107$ differ appreciably in the region between $1.01f_o$ to $1.04f_o$. In this case the method used to measure Q_o at these high frequencies was subject to high percentage error which is responsible for this wide deviation. The capcity c also has a small contribution to this difference. The experimental curve for $Q_o = 107$ is slightly displaced towards the right. This is probably the result of a small error in the determination of the exact resonant frequency since the minimum transmission occurred over a narrow band rather than at one definite frequency. Moreover, this experimental curve does not pass through zero transmission at resonance; this is due to the R.F. oscillator harmonics which were not suppressed at resonance of the fundamental.

Table XIII.

Theoretical Data, Circuit 1.

$Q_o = 13, \; k = 1.$

γ	$\gamma/1-\gamma^2$	$A = \frac{\gamma}{1-\gamma^2} \cdot \frac{2}{13}$	$1+A^2$	$T\% = \frac{100}{\sqrt{1+A^2}}$	$\theta = -\tan^{-1} A.$
0.7	1.37	0.211	1.044	98.0	-11.9°
0.8	2.22	0.342	1.117	~~97.4~~ 94.7	-18.8°
0.9	4.74	0.728	1.517	81.3	-36°
0.92	5.94	0.903	1.815	74.3	-42.1°
0.94	8.1	1.245	2.55	62.6	-51.2°
0.96	12.3	1.89	4.58	46.7	-62.1°
0.98	24.5	3.78	15.3	25.6	-75.2
1.0	∞	∞	∞	0	±90°.
1.02	-25.5	-3.92	16.4	24.7	75.7°
1.04	-13.0	-2.0	5.0	44.6	63.4°
1.06	-8.85	-1.36	2.85	59.1	53.7°
1.08	-6.76	-1.04	2.08	69.4	46.1°
1.1	-5.24	-0.807	1.65	77.8	39°
1.2	-2.73	-0.42	1.18	92.0	22.7°
1.3	-1.88	-0.29	1.084	96.0	16.2°
1.4	-1.46	-0.225	1.05	98.0	12.5°

Table XIV.

Circuit 1.

Theoretical Data

$Q_o = 107$, $k = 1$.

r	$\frac{r}{1-r^2}$	$A = \frac{r}{1-r^2}\frac{2}{107}$	$1+A^2$	$T\% = \frac{100}{\sqrt{1+A^2}}$	$\theta = -\tan^{-1} A$
0.8		.0415			-2.45
0.9	4.74	.0.885	1.008	100	-4.88
0.94	8.1	? 0.151	1.023	98.8	-8.53°
0.96	12.3	0.23	1.053	97.5	-12.97°
0.98	24.5	0.457	1.209	90.9	-27.2°
0.99	49.5	0.925	1.856	73.5	-42.8°
1.0	00	00	00	0.	±90°
1.01	-50.5	-0.942	1.887	72.7	43.4°
1.02	-25.5	-0.476	1.227	90.8	25.5°
1.04	-13.0	-0.243	1.059	97.0	13.7°
1.06	- 8.85	-0.165	1.027	98.7	9.4°
1.08	- 6.76	-0.126	1.016	99.3	7.2°
1.1	- 5.24	-0.98	1.009	100	5.6°
1.2		? 0.051			2.9

TRANSMISSION AND PHASE-SHIFT CHARACTERISTICS, CIRCUIT 1.

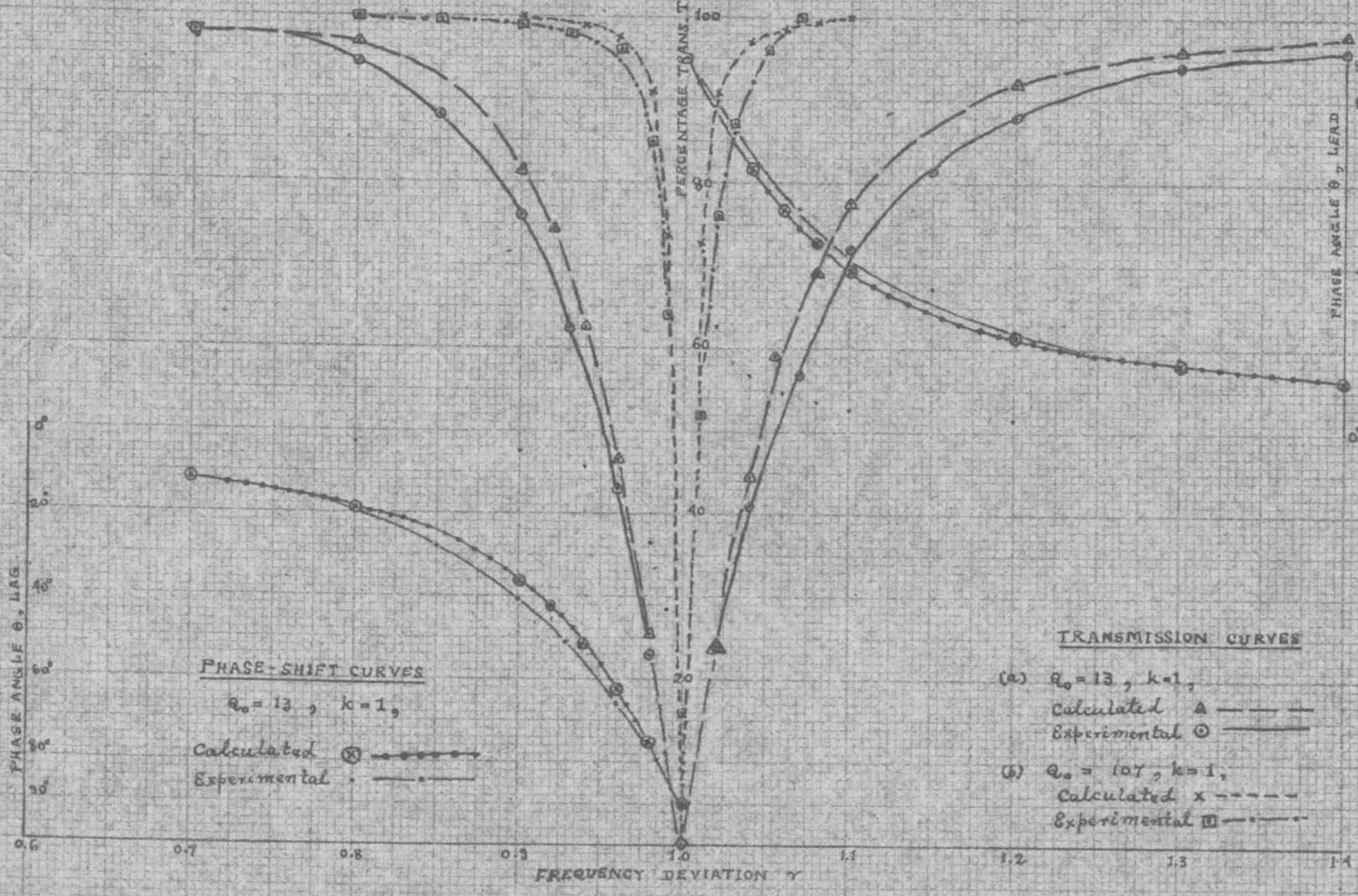

Fig. 13.

The transmission characteristics shown in Figs. 9 and 11 obtained from experiment, clearly indicate that higher values of Q_o result in higher circuit selectivity. The phase-shift curves in Fig. 10 show that higher Q_o also leads to less phase shift at frequencies off resonance. Figure 12 indicates that greater values of k lead to higher selectivity. These results are exactly in agreement with the theoretical conclusions on page 12. Of course for figure 12, higher values of k were accompanied by slightly lower Q_o due to smaller resonant frequency; yet the improvement in selectivity is quite noticeable. If Q_o was kept fixed for the different values of k, the curves would show more selectivity as k was made larger. This agreement between the theoretical and experimental results verifies Eq. 17.

In the high frequency region the phase angles could not be measured because the R.F oscillator contained appreciable harmonics which, together with extraneous disturbances, produced patterns on the oscilloscope screen that were of very irregular shape.

Experiment on circuit 2.

Experiments on this circuit, Fig. 5, were conducted to determine the transmission and phase shift characteristics for different values of Q (defined as a pure ratio of the reactance of the coil and the resistance of R_p) and k, in the low frequency region between 850 cycles and 50 kc. Circuit parameters were so chosen as to make a suitable compromise between circuit selectivity and loading. The shunting resistance R_p and the bridging resistance R had different values for each value of Q_o used. In each case R_p was first selected to give the desired Q_o and then the value of R was finally adjusted during experiment until the circuit transmission was exactly nill at resonance. At this point the resonant condition as given by Eq. 28 was satisfied.

The inductance of the coil and the resistance R_p were measured at 1000 cycles by an impedance bridge. Q_o was computed from the relation, $Q_o = 2\pi f_o L_p / R_p$.

Experimental procedure was exactly the same as before. Results of these measurements are given in tables XV to XXI, and the corresponding curves are shown by figures 14 to 17.

Table XV.

Circuit 2.

L_p = 5.25 mh. C=C/k = 0.02 μF. R_p = 370 ohms.

f_o = 11.25 kc. k = 1.

Q_o = 1.

		Transmission			Phase angle E_{in} = 3 volts.			
γ	f kc	E_{in}	E_{out}	T%	2b	2a	b/a	θ
0.1	1.125	10 v	9.8 v	98.0	3.0	17	0.176	10.2°
0.2	2.25	"	9.3	93.0	5.4	16	0.348	19.7°
0.4	4.5	"	7.4	74.0	8.0	12.5	0.64	39.8°
0.6	6.75	"	4.8	48.0	7.45	8.55	0.875	61°
0.8	9.0	"	2.2	22.0	9.0	9.4	0.958	76.5°
0.9	10.125	"	1.1	11.0	..	..	..	..
1.0	11.25	"	0.005	0.5	..	..	..	±90°
1.1	12.38	"	0.9	9.0	..	..	..	..
1.2	13.5	"	1.75	17.5	6.0	6.6	0.947	71.2°
1.4	15.75	"	3.15	31.5	9.7	12.0	0.81	54.1°
1.6	18.0	"	4.35	43.5	10.6	15.3	0.692	43.8°
1.8	20.3	"	5.5	55.0	11.9	18.9	0.63	39°
2.0	22.5	"	6.1	61.0	12.4	21.0	0.59	36.2°

Table XVI.

Circuit 2.

L_p = 5.25 mh. C=C/k = 0.02 μF. R_p = 740 ohms.

f_o = 11.25 kc. k = 1.

Q_o = 0.5.

		Transmission			Phase angle E_{in} = 3 volts.			
γ	f kc	E_{in}	E_{out}	T%	2b	2a	b/a	θ
0.1	1.125	10 v	9.9 v	99	2.1	19	0.11	6.3°
0.2	2.25	"	9.75	97.5	3.7	18.5	0.2	11.5°
0.4	4.5	5 v	4.45	89	7.2	17.6	0.408	24.1°
0.6	6.75	"	3.65	73	9.0	13.8	0.652	40.7°
0.8	9.0	"	2.0	40	6.8	7.8	0.87	60.5°
1.0	11.25	"	0	0	..	..	..	±90°
1.2	13.5	"	1.8	36	11.5	13.4	0.86	59.3°
1.4	15.75	"	2.9	58	15.5	21.5	0.722	46.2°
1.6	18.0	"	3.6	72	15.8	26.5	0.596	36.5°
1.8	20.3	"	4.0	80	14.1	29.3	0.48	28.8°
2.0	22.5	"	4.25	85	12.8	30.4	0.421	24.8°

Table XVII.

Circuit 2.

L_p = 5.25 mh. C=C/k = 0.005 μF. R_p = 3,720 ohms.

f_o = 22.3 kc. k = 1 R = 575 ohms.

Q_o = 0.2.

		Transmission			Phase angle E_{in} = 3 v.			
γ	f kc	E_{in}	E_{out}	T%	2b	2a	b/a	θ
0.1	2.23	5 v	5 v	100	1.1	13.5	0.082	4.7°
0.2	4.46	"	4.98	98.6	1.7	13.4	0.127	7.6°
0.4	8.92	"	4.85	97.0	3.2	12.8	0.25	14.5°
0.6	13.38	"	4.5	90.0	5.1	12.0	0.425	25.2°
0.8	17.84	"	3.4	68.0	6.7	9.0	0.745	48.2°
1.0	22.3	"	0	0	..	..	..	±90°
1.2	26.8	"	3.15	63.0	6.3	8.4	0.75	48.5°
1.4	31.2	"	4.18	83.6	5.8	10.5	0.555	33.5°
1.6	35.6	"	4.52	90.4	4.7	11.4	0.412	24.4°
1.8	40.2	"	4.7	94.0	4.0	13.8	0.29	16.9°
2.0	44.6	"	4.8	96.0	2.5	12.0	0.308	12°

Table XVIII.

Circuit 2.

L_p = 5.25 mh. $C=C/k$ = 0.005 μF. R_p = 370 ohms.

f_0 = 22.3 kc. k = 1. R = 5,350 ohms.

Q_0 = 2.

		Transmission			Phase angle E_{in} = 3v			
γ	f kc	E_{in}	E_{out}	T%	2b	2a	b/a	θ
0.1	2.23	5v	4.59 v	91.8	6.0	13.6	0.442	26.2°
0.2	4.46	"	3.82	76.4	7.0	11.0	0.636	39.5°
0.4	8.92	"	2.32	46.2	11.5	12.9	0.892	63.1°
0.6	13.38	"	1.27	25.4	6.85	7.0	0.98	78.5°
0.8	17.84	"	0.05	10.0	3.8	3.85	0.996	84.9°
1.0	22.3	"	0	0	...	..	...	±90°
1.2	26.8	"	0.04	8.0	2.8	2.9	0.965	74.6°
1.4	31.2	"	0.08	16.0	4.6	5.0	0.92	66.9°
1.6	35.6	"	1.15	23.0	6.0	6.9	0.87	60.3°
1.8	40.2	"	1.4	28.0	7.1	8.7	0.816	54.7°
2.0	44.6	"	1.7	34.0	4.0	5.1	0.785	51.7°

TRANSMISSION CHARACTERISTICS, CIRCUIT 2, CONSTANT $k = 1$.

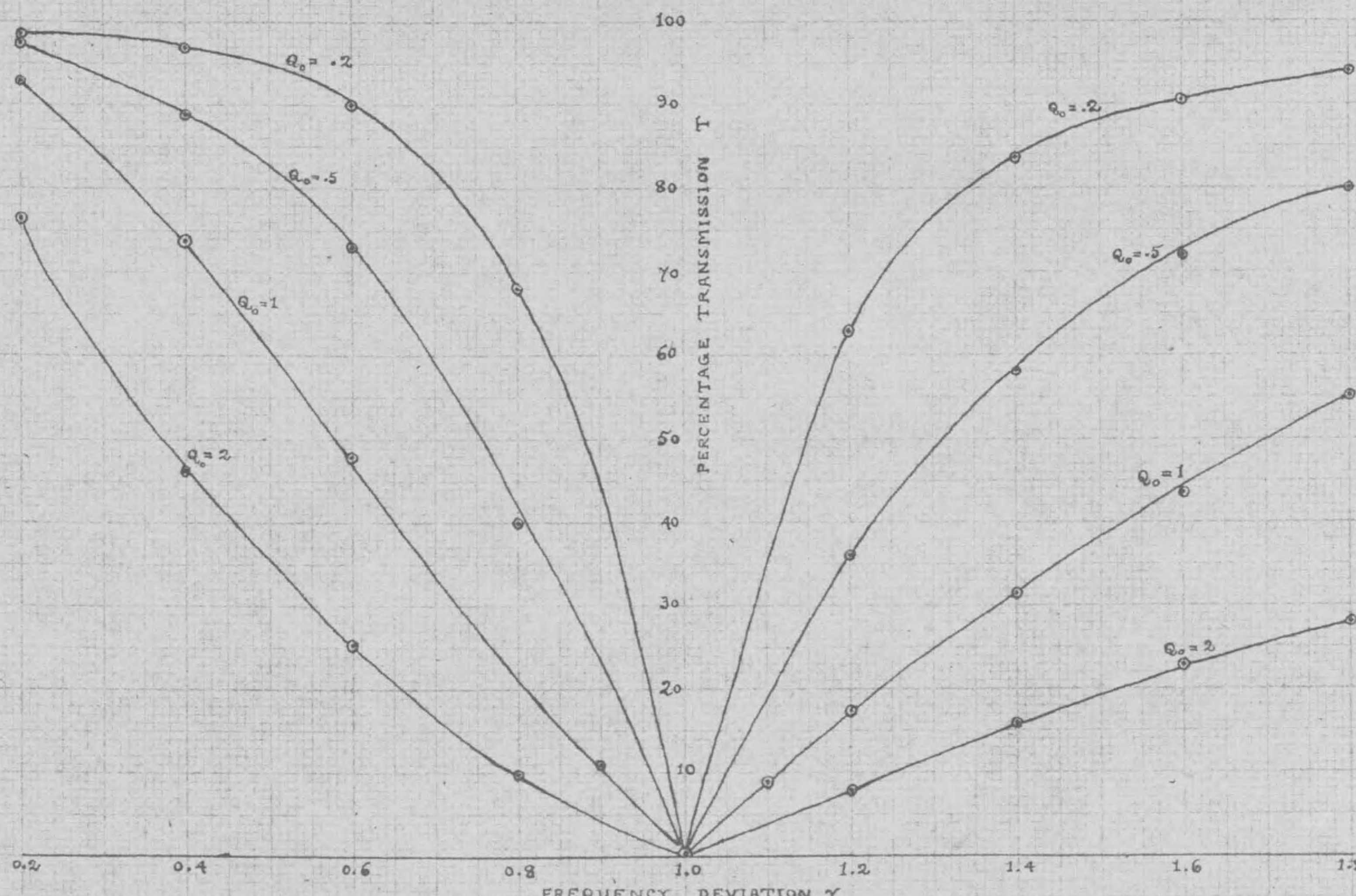

Fig. 14.

PHASE-SHIFT CHARACTERISTICS, CIRCUIT 2,
CONSTANT k=1.

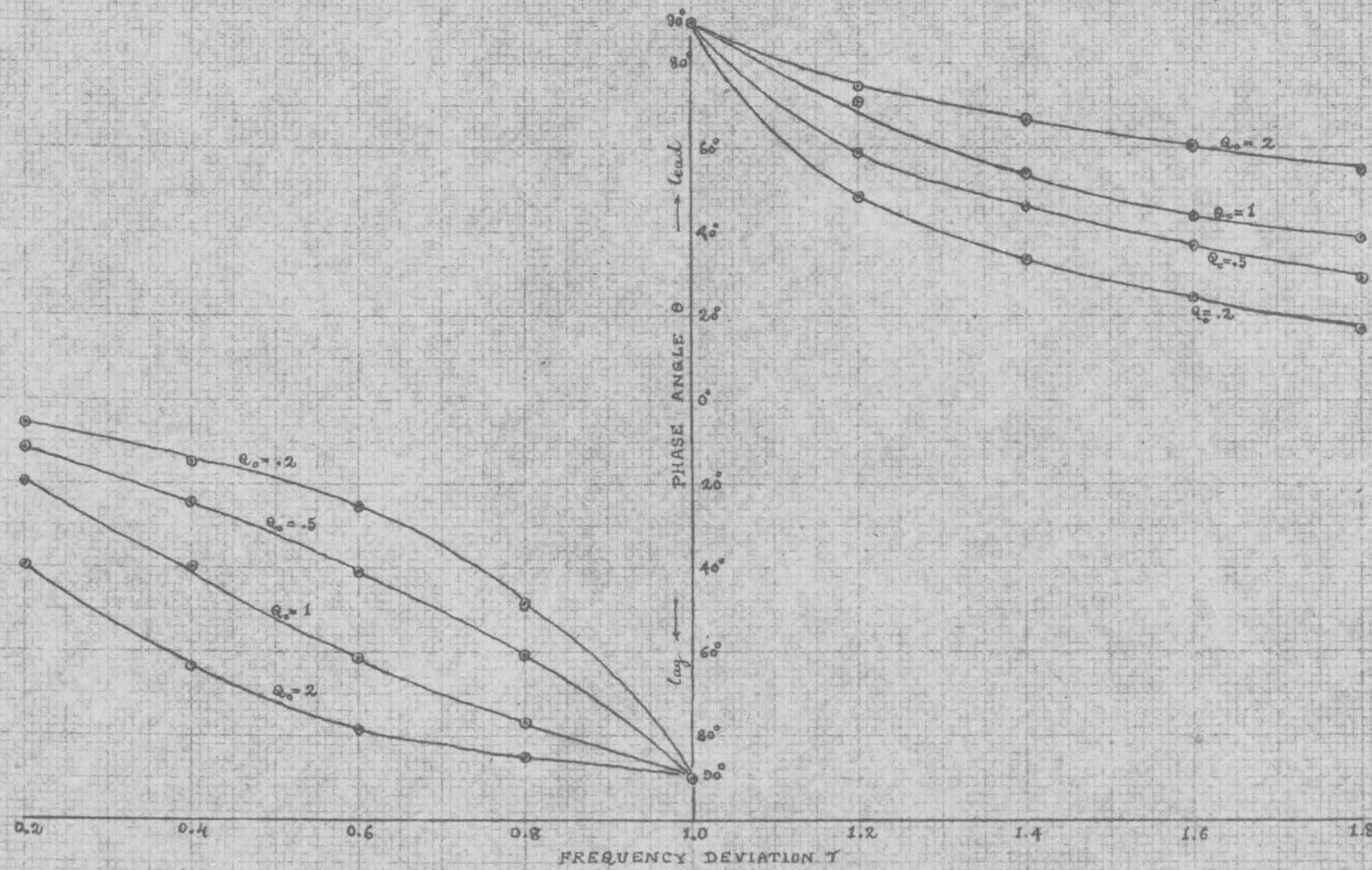

Fig. 15.

Table XIX.

Circuit 2.

$L_p = 5.25$ mh.

$f_o = 8.95$ kc.

$C = 0.02\ \mu F$.

$C/k = 0.422\ \mu F$.

$Q_o = 0.398$.

$k = 0.476$.

$R_p = 740$ ohms.

$R = 525$ ohms

		Transmission			Phase angle $E_{in} = 3$ v.			
γ	f kc.	E_{in}	E_{out}	T%	2b	2a	b/a	θ
0.1	0.895	5 v	4.98 v	99.6	1.8	13.1	0.138	7.8°
0.2	1.79	"	4.82	96.4	3.4	12.8	0.266	15.4°
0.4	3.58	"	4.3	86.	5.5	11.2	0.49	29.4°
0.6	5.37	"	3.27	65.4	6.4	8.7	0.735	47.3°
0.8	7.16	"	1.75	35.	4.3	4.7	0.915	66.2°
1.0	8.95	"	0	0	..	..	..	±90°
1.2	10.75	"	1.4	28.	3.6	3.8	0.947	72.5°
1.4	12.53	"	2.38	47.6	5.3	6.4	0.83	56.1°
1.6	14.32	"	3.1	62.	6.0	8.0	0.75	48.5°
1.8	16.1	"	3.5	70.	6.2	9.3	0.667	41.8°
2.0	17.9	"	3.82	76.4	6.2	10.1	0.613	37.8°

Table XX.

Circuit 2.

$L_p = 5.25$ mh. $C = 0.02\ \mu F$. $R_p = 740$ ohms.

$f_0 = 13.2$ kc. $C/k = 0.01\ \mu F$. $R = 1,050$ ohms.

$Q_o = 0.586$.

$k = 2$.

		Transmission			Phase angle $E_{in} = 3v$			
γ	f kc	E_{in}	E_{out}	T%	2b	2a	b/a	θ
0.1	1.36	10 v	9.95 v	99.5	1.8	17.1	0.15	6.1°
0.2	2.64	"	9.8	98	3.5	17.5	0.2	11.6°
0.4	5.28	"	9.2	92	6.3	15.8	0.398	23.3°
0.6	7.92	"	7.5	75	8.3	13.0	0.639	39.7°
0.8	10.56	5 v	2.15	43	6.6	7.4	0.892	63.1°
1.0	13.2	"	0.005	1	..	..	..	±90°
1.2	15.85	"	2.1	4 2	6.3	7.1	0.887	62.5°
1.4	18.50	"	3.1	62	9.5	12.8	0.742	47.9°
1.6	21.11	"	3.6	72	13.7	21.0	0.679	42.7°
1.8	23.8	"	4.2	84	10.8	21.4	0.505	30.3°
2.0	26.4	"	4.4	88	9.1	20.8	0.437	25.9°

Table XXI.

Circuit 2.

$L_p = 5.25$ mh. $C = 0.02\ \mu F.$ $R_p = 740$ ohms.

$f_o = 14.3$ kc. $C/k = 0.005\ \mu F.$ $Q_o = 0.635.$

$k = 4.$

		Transmission			Phase angle $E_{in} = 3$ v.			
γ	f kc	E_{in}	E_{out}	T%	2b	2a	b/a	θ
0.1	1.43	5 v	4.95 v	99	1.5	13.6	0.11	6.3°
0.2	2.86	"	4.9	98	2.5	13.6	0.184	10.6°
0.4	5.72	"	4.65	93	4.6	12.7	0.362	21.2°
0.6	8.58	"	3.98	79.6	6.6	11.0	0.6	36.8°
0.8	11.43	"	2.35	47	5.7	6.7	0.85	58.3°
1.0	14.3	"	0	0	--	--	--	±90°
1.2	17.15	"	2.1	42	4.9	5.7	0.86	59.3°
1.4	20	"	3.23	64.6	6.3	9.0	0.7	44.5°
1.6	22.85	"	3.9	78	5.8	9.7	0.597	36.7°
1.8	25.7	"	4.2	84	5.2	10.6	0.49	29.4°
2.0	28.6	"	4.4	88	4.8	10.7	0.448	26.4°

TRANSMISSION CHARACTERISTICS, CIRCUIT 2.

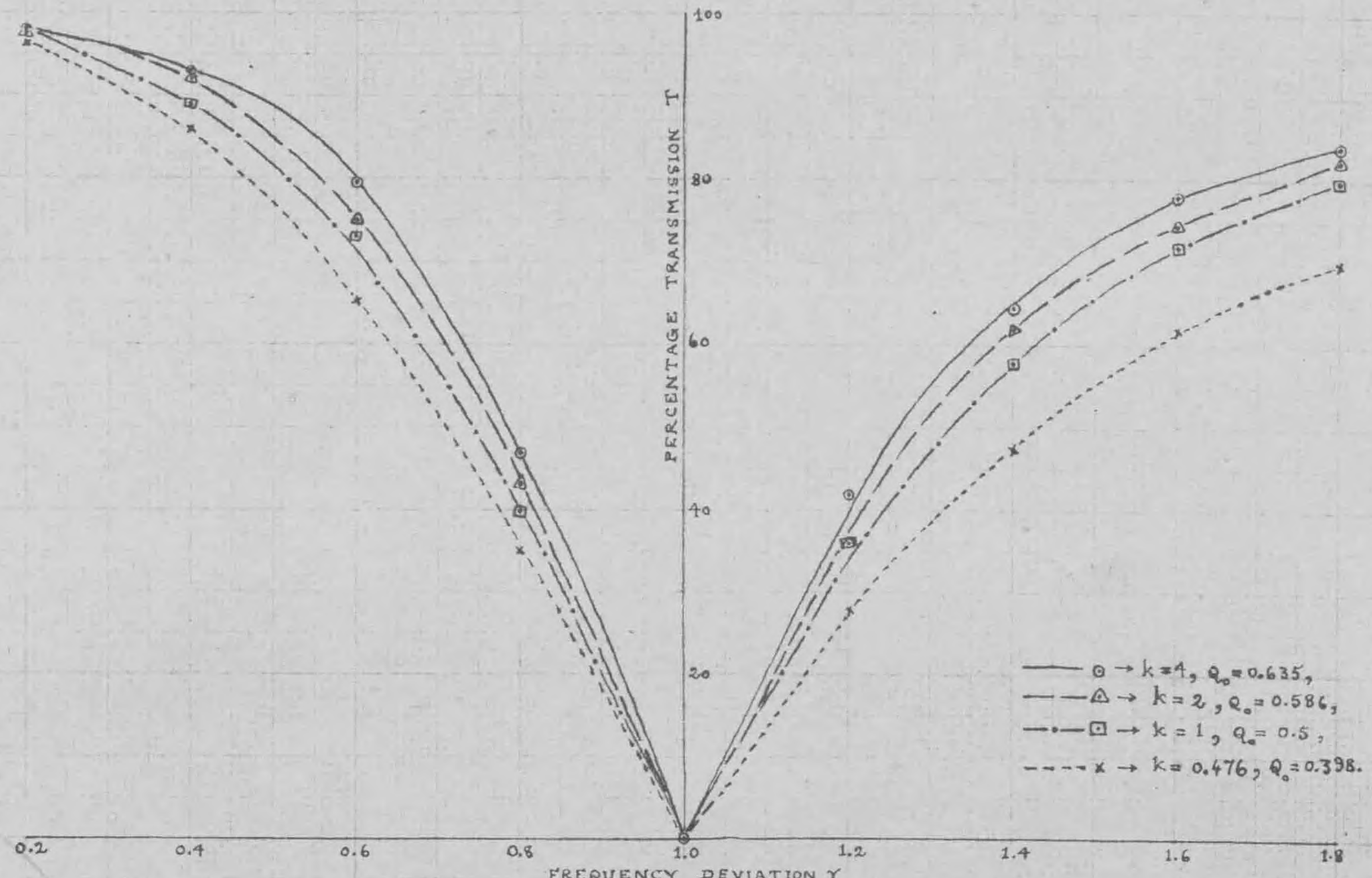

Fig. 16.

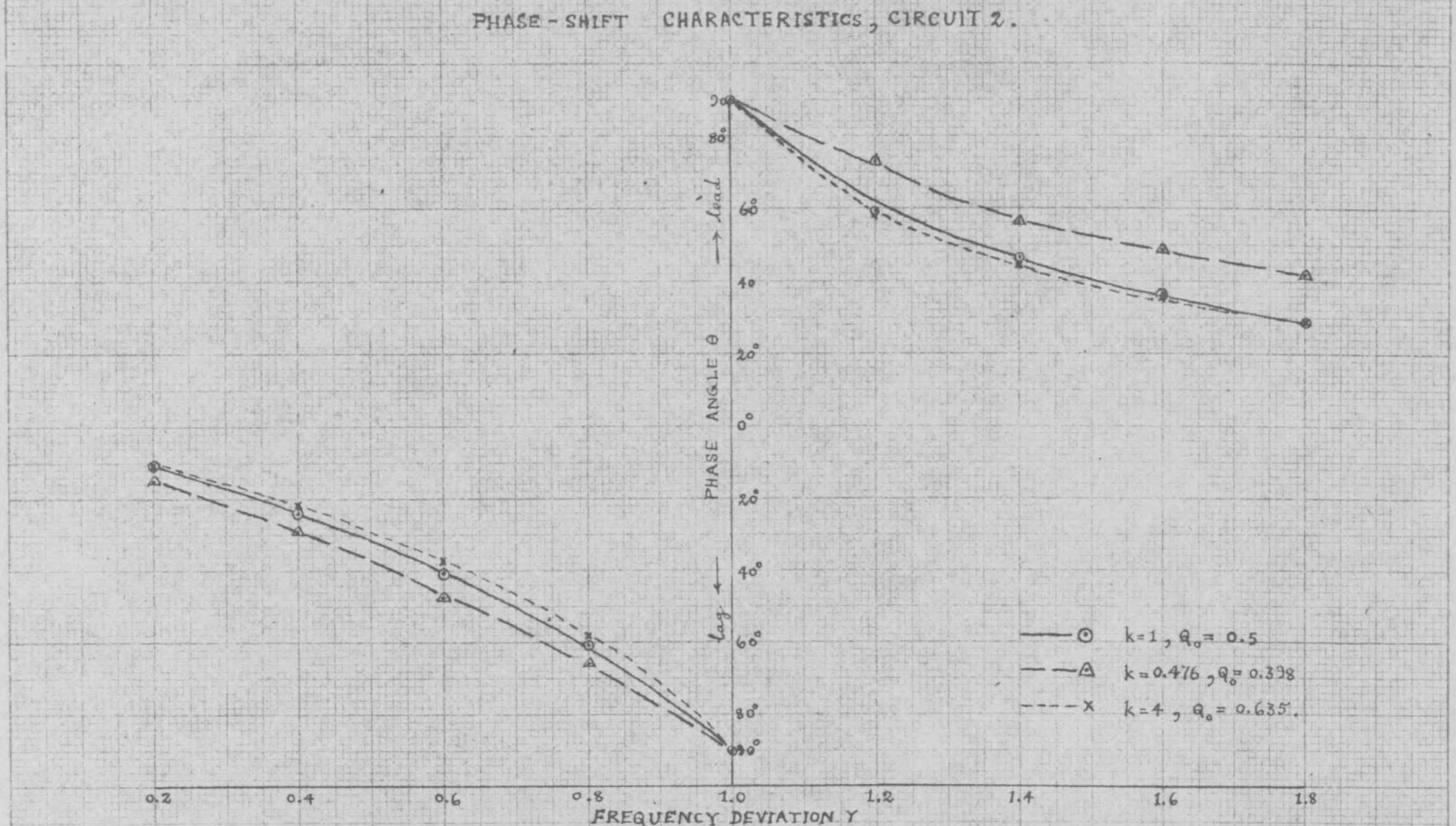
PHASE - SHIFT CHARACTERISTICS, CIRCUIT 2.
90°
80°
→ lead
60°
40°
20°
PHASE ANGLE θ
0°
20°
40°
← lag
60°
80°
90°
0.2
0.4
0.6
0.8
1.0
1.2
1.4
1.6
1.8
FREQUENCY DEVIATION γ
k=1, Q₀= 0.5
k=0.476, Q₀= 0.398
k=4, Q₀= 0.635.

Fig. 17.

Discussion.

At this point a comparison of the experimental results and the theoretical derivations will be made. Resonant frequencies of the circuits used were calculated from Eq. 29, and the values of R that correspond to null transmission at resonance were evaluated from Eq. 28. The calculated and experimental values are given below for comparison. The experimental values of R shown in the table XXIII were measured by the use of an ohmmeter contained in a commercial multimeter. Hence the measured values of R were not determined with great accuracy.

TABLE XXII.

Comparison of resonant frequencies.

Reference to table	Calculated values	Experimental values
XV, XVI	10.98 kcs.	11.25 kcs.
XVII, XVIII	22.0 "	22.3 "
XIX	8.82 "	8.95 "
XX	12.7 "	13.2 "
XXI	13.9 "	14.3 "

Table XXIII.

Comparison of the Values of R.

Reference to table	Calculated values	Experimental values
XVII	547 ohms	575 ohms
XVIII	5,505 "	5,350 "
XIX	535 "	525 "
XX	982	1,050 "

Comparison of the resonant frequencies in table XXII reveals that there is good agreement between the calculated and experimental results; and the resonant condition given by Eq. 29 is verified. The slight difference between the two is due to errors in accurate determination of L_p and C. In table XXIII, the values of R agree fairly well and hence verify the resonant condition given by Eq. 28, the difference being due largely to an inaccurate determination of R.

In this case also, capacities smaller than 0.003μF were not used in the circuits because then the effect of c, the stray capcity of the junction point, was noticeable in altering the circuit performance.

The transmission and phase shift characteristics of the circuit can be calculated from Eqs. 31 and 32, respectively. Such calculations are shown in tables XXIV to XXVI. The calculated points are plotted in figures 18 and 19.

Comparison of the experimental and calculated transmission characteristics in Fig. 18 shows excellent agreement. Hence Eq. 31 is fully verified.

The phase shift curves in Fig. 19 show close correspondence between the theoretical and experimental results only for frequencies below the resonant frequency. At frequencies above the resonant frequency the experimental curves deviate considerably from their corresponding theoretical curves. The reason for such a wide divergence is quite obscure. However, at the higher frequencies the small capacity c has a contribution, but not to such an extent revealed by the comparison.

Table XXIV.

Theoretical Data, Circuit 2.

$Q_o = 1, \quad k = 1.$

γ	$\frac{\gamma}{1-\gamma^2}$	$A = \frac{\gamma}{1-\gamma^2} \cdot 2$	$1 + A^2$	$T\% = \frac{100}{\sqrt{1+A^2}}$	$\theta = -\tan^{-1} A$
0.1	0.102	0.204	1.042	98.	-11.5°
0.2	0.208	0.416	1.17	92.6	-22.5°
0.4	0.477	0.954	1.91	72.4	-43.7°
0.6	0.937	1.87	4.5	47.2	-61.9°
0.8	2.22	4.44	20.7	21.9	-77.3°
1.0	00	00	00	0	±90°
1.2	-2.73	-5.46	30.8	18 .	79.6°
1.4	-1.46	-2.92	9.5	32.4	71.1°
1.6	-1.025	-2.05	5.2	44.2	64.1°
1.8	-0.804	-1.61	3.59	53.5	58.1°
2.0	-0.666	-1.33	2.78	59.8	53.1°

Table XXV.

Theoretical Data, Circuit 2.

$Q_o = 0.5, \quad k = 1.$

γ	$\frac{\gamma}{1-\gamma^2}$	$A = \frac{\gamma}{1-\gamma^2} \cdot 1$	$1 + A^2$	$T\% = \frac{100}{\sqrt{1+A^2}}$	$\theta = -\tan^{-1} A$
0.1	0.102	0.102	1.01	100	-5.8°
0.2	0.208	0.208	1.043	98.	-11.7°
0.4	0.477	0.477	1.227	90.	-25.5°
0.6	0.937	0.937	1.87	73.5	-43.2°
0.8	2.22	2.22	5.92	41.	-65.7°
1.0	00	00	00	0	$\pm 90^\circ$
1.2	-2.73	-2.73	8.45	34.5	69.7°
1.4	-1.46	-1.46	3.13	56.5	55.5°
1.6	-1.025	-1.025	2.04	70.	45.5°
1.8	-0.804	-0.804	1.64	78.	38.8°
2.0	-0.666	-0.666	1.44	83.	33.7°

Table XXVI.

Theoretical Data, Circuit 2.

$Q_o = 2$, $k = 1$.

γ	$\frac{\gamma}{1-\gamma^2}$	$A = \frac{\gamma}{1-\gamma^2}4$	$1 + A^2$	$T\% = \frac{100}{\sqrt{1+A^2}}$	$\theta = -\tan^{-1}A$
0.1	0.102	0.408	1.166	92.6	-21.7°
0.2	0.208	0.832	1.69	76.9	-39.8°
0.4	0.477	1.91	4.6	46.7	-62.4°
0.6	0.937	3.74	15.0	25.7	-75°
0.8	2.22	8.88	79.7	11.2	-83.6°
1.0	∞	∞	∞	0	±90°
1.2	-2.73	-10.92	121.	9.	84.8°
1.4	-1.46	-5.84	35.	16.9	80.4°
1.6	-1.025	-4.1	17.8	23.2	76.3°
1.8	-0.804	-3.22	11.3	29.7	72.7°
2.0	-0.666	-2.66	8.2	35.2	69.4°

TRANSMISSION CHARACTERISTICS, CIRCUIT 2.

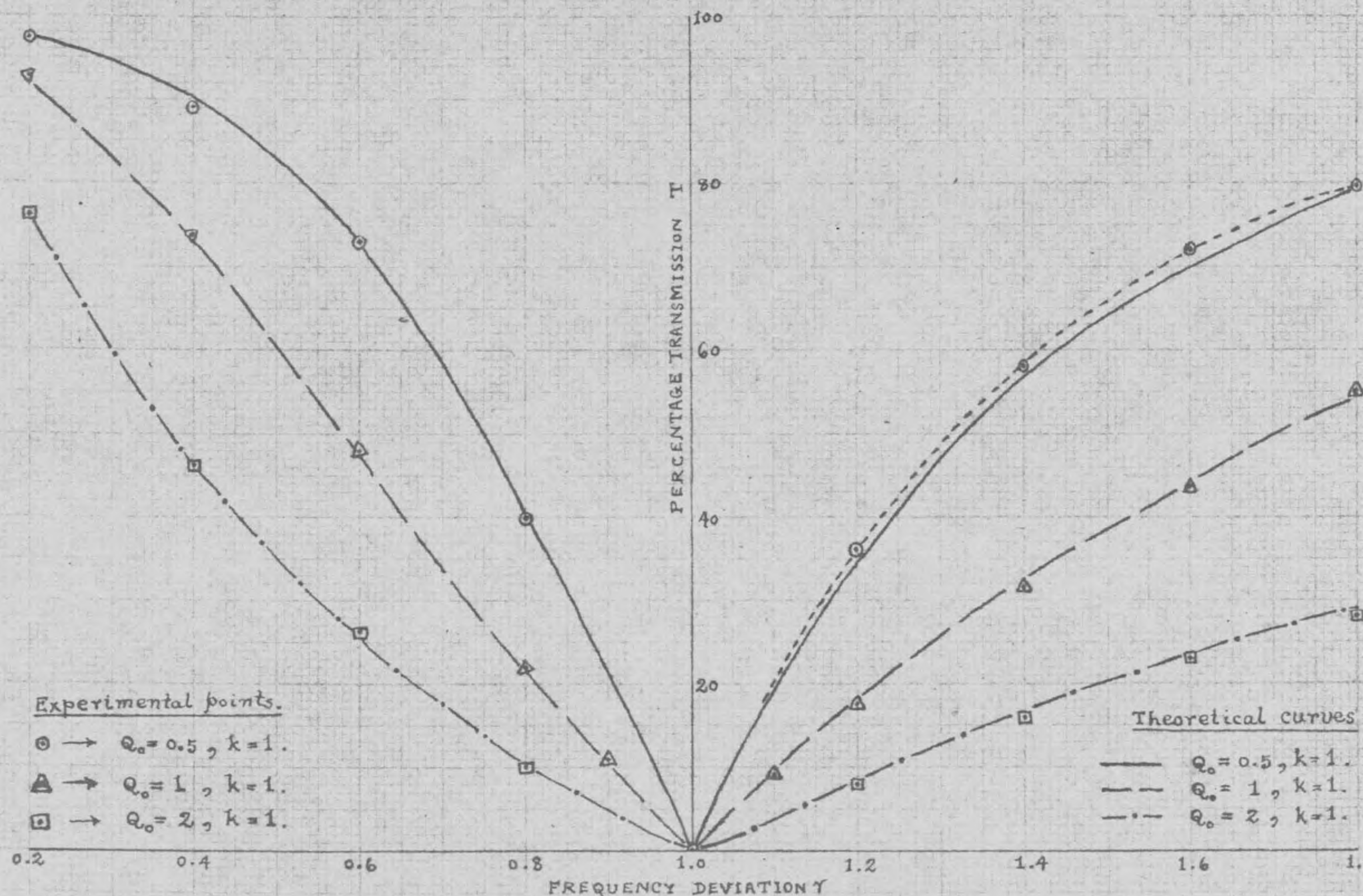

Fig. 18.

PHASE - SHIFT CHARACTERISTICS , CIRCUIT 2.

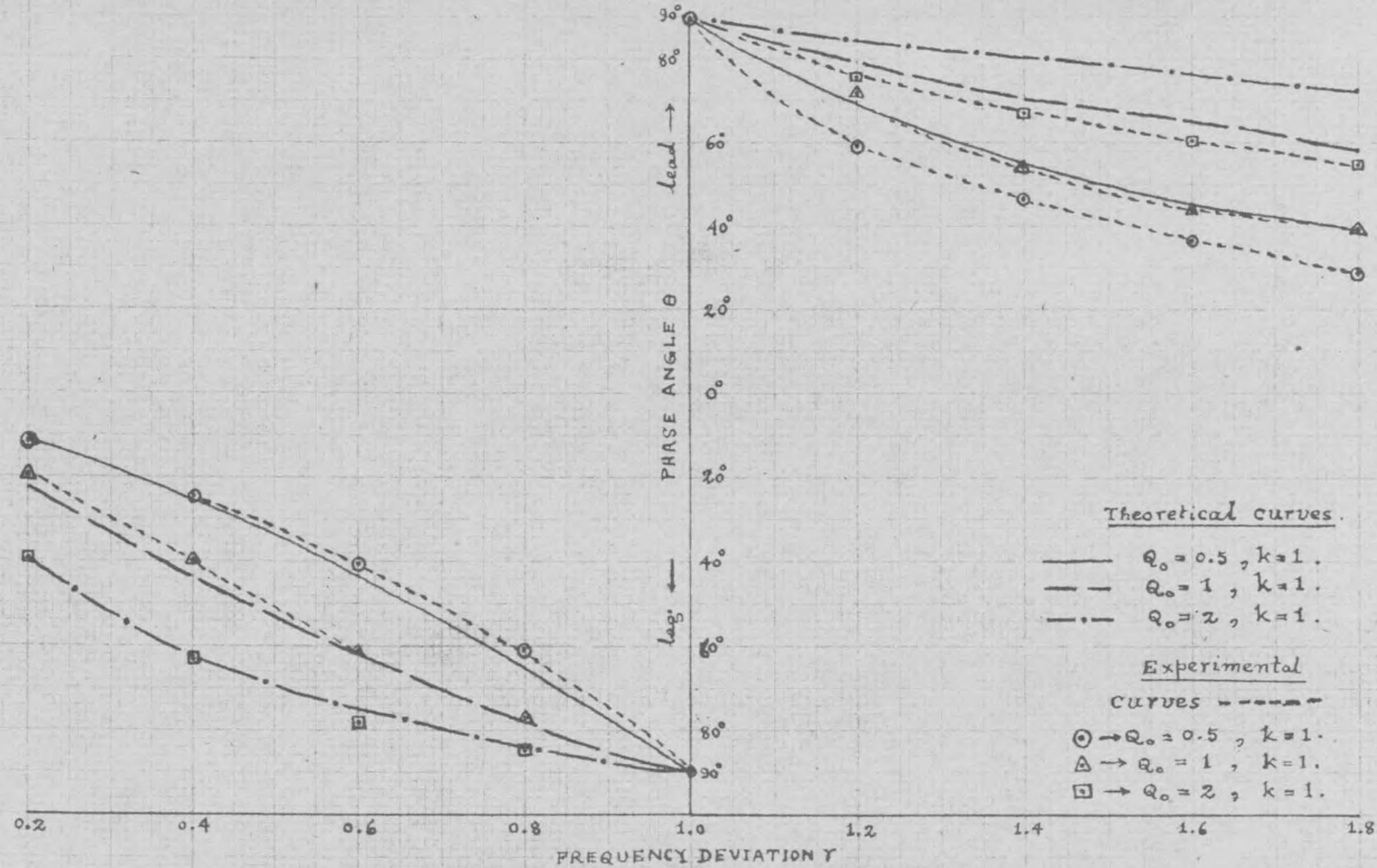

Fig. 19.

The transmission characteristics shown in Fig. 14 clearly indicate that smaller values of Q_o yield greater selectivity. Also, higher values of Q_o produce less phase shift at frequencies off resonance as is indicated by the curves in Fig. 15. The curves of Fig. 16 show that higher values of k produce higher selectivity. These results are in exact agreement with the theoretical conclusions on page 16. Of course for Fig. 16 higher values of k were accompanied by increased values of Q_o so that the improvement in selectivity was slightly masked by increases in Q_o. In Fig. 17, with the increase of k the corresponding increase in Q_o was such that the improvement in phase shift is only slightly noticeable. If Q_o was held fixed and k increased, higher selectivity and less phase shift would be more distinct for higher values of k, as concluded from theory.

It was intended to extend the present work into the radio frequency region, but many complications arose. For example, the R.F. oscillator harmonics, distributed coil capacity, other stray capacities, etc., disturbed the experiment. In order to conduct experiments in this region, precautions must be taken to minimize and avoid those disturbing effects. Complete elimination of these effects would require a separate study; consequently experimentation in this range is incomplete and is omitted from this paper.

Summary and Conclusions.

The investigation of the bridged-T networks was based on a sound mathematical theory developed in a perfectly generalized way. Though only two typical circuits were selected for experiments, the theory is quite general and could be applied to any bridged-T network and its characteristics determined theoretically. The discussions covered both the symmetrical and nonsymmetrical circuits, including the determination of all their characteristics excepting the actual measurement of the input and output impedances. The theoretical conclusions were well supported by experimental results.

The circuit selectivity and phase shift characteristics can be easily controlled by variation of circuit parameters. The component values were always so chosen as to make a compromise between selectivity and loading of the circuit. In order to avoid the effect of stray capacity, the circuit capacitors were large compared with the stray capacitances.

The most salient feature of bridged-T networks is their infinite attenuation or zero transmission at the resonant frequency though considerable dissipation exists in some of the components. In contrast to an antiresonant wave trap, where the impedance simply passes through its maximum at resonance, the resonant impedance of bridged-T circuits becomes infinite. This holds even for low audio frequencies. In order to have such high resonant impedances in the audio frequency region by a parallel resonant circuit, a huge coil of impracticable size would be needed.

These circuits have selective response over a band of frequencies about the resonant frequency, the desired characteristics being obtainable by proper choice of Q and k. The unsymmetrical circuits with higher values of k yield better selectivity and less phase shift at frequencies off resonance. In view of this selective response property, these circuits can be used as wave filters having the desired frequency response over the desired band. They can also be used as feed-back circuits in which case they must have the required frequency response and phase shift characteristics over the desired frequency range.

In operation these circuits are very simple, the generator and the load being connected directly across the input and output, respectively. The input and output terminals have a common ground, consequently coupling transformer or Wagner earth connections are not required. However, care should be taken to eliminate direct coupling between the source and the load and also to avoid the effect of unwanted capacities. One of the disadvantages of these circuits is that, unlike antiresonant wave traps, they load both the source and the detector across which they are inserted and hence have insertion loss.

In view of their perfect null transmission at the resonant frequency, bridged-T circuits can be used as wave traps for absolute suppression of any single frequency where the frequency to be filtered corresponds to the resonant frequency of the circuit. They are unsuitable for filtering a supply containing many different frequencies since these circuits will suppress only a very narrow band of frequencies due to their high selectivity.

They can also be used as bridge measuring instruments for measuring inductance, capacitance, resistance, dielectric constant, quality factor and unknown frequencies. In these applications very little attention need be paid to circuit characteristics except to obtain a perfect null at the desired balance point.

List of literature cited.

1. Everitt, W. L., COMMUNICATION ENGINEERING, Second Edition, pp 38, McGraw Hill Book Co., New York.

2. Reed, M. B., GENERAL FORMULAS FOR T AND Π-NETWORK EQUIVALENTS, Proc. I.R.E., pp 897, December, 1945.

3. Schulz, E. H., and Anderson, L. T., EXPERIMENTS IN ELECTRONICS AND COMMUNICATION ENGINEERING, pp 165, Harper Co., New York.

4. Stanton, L., THEORY AND APPLICATION OF PARALLEL-T RESISTANCE CAPACITANCE FREQUENCY SELECTIVE NETWORKS, Proc. I.R.E., pp 447, July, 1946.

5. Terman, F. E., RADIO ENGINEER'S HANDBOOK, First Edition, pp 918, McGraw-Hill Book Co., New York, 1943.

6. Terman, F. E., RADIO ENGINEERING, Second Edition, pp 212, McGraw-Hill Book Co., New York, 1937.

7. Tuttle, W. N., BRIDGED-T AND PARALLEL-T CIRCUITS FOR MEASUREMENTS AT RADIO FREQUENCIES, Pro. I.R.E., pp 23, January, 1940.

Appendix.

1. General Theory.

Let E_1 represent the impressed input voltage and E_2 the output voltage of the bridged-T circuit shown in Fig. 1. The disposition of the component impedances and the polarity of the voltages are as indicated in the figure. Applying Kirchhoff's laws to the different meshes of the circuit, the voltage and current relations become

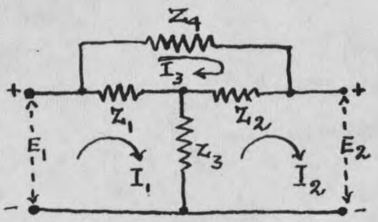

Fig. 1.

$$E_1 = (Z_1+Z_3)I_1 - Z_3I_2 - Z_1I_3. \quad ...... \quad 1a.$$

$$-E_2 = -Z_3I_1 + (Z_2+Z_3)I_2 - Z_2I_3 \quad ...... \quad 1b.$$

$$0 = -Z_1I_1 - Z_2I_2 + (Z_1+Z_2+Z_4)I_3. \quad ...... \quad 1c.$$

Placing them in matrix form,

$$\begin{Vmatrix} E_1 \\ -E_2 \\ 0 \end{Vmatrix} = \begin{Vmatrix} Z_1+Z_3 & -Z_3 & -Z_1 \\ -Z_3 & Z_2+Z_3 & -Z_2 \\ -Z_1 & -Z_2 & Z_1+Z_2+Z_4 \end{Vmatrix} \begin{Vmatrix} I_1 \\ I_2 \\ I_3 \end{Vmatrix}$$

If D, the determinant of the impedance matrix, is not zero (which will hold true under all the circumstances to be considered), the matrix may be inverted into the form

$$\begin{Vmatrix} I_1 \\ I_2 \\ I_3 \end{Vmatrix} = \frac{1}{D}\begin{Vmatrix} d_{11} & d_{12} & d_{13} \\ d_{21} & d_{22} & d_{23} \\ d_{31} & d_{32} & d_{33} \end{Vmatrix} \begin{Vmatrix} E_1 \\ -E_2 \\ 0 \end{Vmatrix} \quad 2.$$

where, d_{ij} =(the cofactor of the ith row and jth column of D)= d_{ji} .

Therefore,

$$D = \begin{vmatrix} Z_1+Z_3 & -Z_3 & -Z_1 \\ -Z_3 & Z_2+Z_3 & -Z_2 \\ -Z_1 & -Z_2 & Z_1+Z_2+Z_4 \end{vmatrix}$$

$$= Z_4\,(Z_1Z_2 + Z_2Z_3 + Z_1Z_3)\,. \quad \ldots\ldots \quad 3a.$$

$$d_{11} = \begin{vmatrix} Z_2+Z_3 & -Z_2 \\ -Z_2 & Z_1+Z_2+Z_4 \end{vmatrix}$$

$$= Z_1Z_2 + Z_2Z_3 + Z_1Z_3 + Z_2Z_4 + Z_3Z_4\,. \quad 3b.$$

$$d_{12} = d_{21} = -\begin{vmatrix} -Z_3 & -Z_1 \\ -Z_2 & Z_1+Z_2+Z_4 \end{vmatrix}$$

$$= Z_1Z_2 + Z_2Z_3 + Z_1Z_3 + Z_3Z_4\,. \quad \ldots\ldots \quad 3c.$$

$$d_{22} = \begin{vmatrix} Z_1+Z_3 & -Z_1 \\ -Z_1 & Z_1+Z_2+Z_4 \end{vmatrix}$$

$$= Z_1Z_2 + Z_2Z_3 + Z_1Z_3 + Z_1Z_4 + Z_3Z_4\,. \quad \ldots\ldots \quad 3d.$$

1a. Network transmission and resonance.

From the above deductions an expression for the circuit transmission $T = E_2/E_1$, will be derived under conditions of no load. From Fig. 1 it may be seen that no load condition is given by $I_2 = 0$.

From Eq. 2, $$I_2 = \frac{1}{D}\,(d_{21}E_1 - d_{22}E_2)\,.$$

Hence under no load condition, for $I_2 = 0$,

$$d_{21}E_1 - d_{22}E_2 = 0.$$

Therefore, $$T = \frac{E_2}{E_1} = \frac{d_{21}}{d_{22}} = \frac{Z_1Z_2 + Z_2Z_3 + Z_1Z_3 + Z_3Z_4}{Z_1Z_2 + Z_2Z_3 + Z_1Z_3 + Z_3Z_4 + Z_1Z_4}\,. \quad 4.$$

1b. Equivalent Pi-circuit.

In Fig. 2 is shown a Pi-circuit for which the values of the component impedances Z_A, Z_B and Z_C are to be determined in terms of the component impedances Z_1, Z_2, Z_3 and Z_4 of Fig. 1 such that this Pi-circuit may be an equivalent representative of the original bridged-T circuit. It is clear from a comparison of Fig. 1 and Fig. 2 that I_1 is the same as I_A, I_2 is the same as I_B, but $I_3 \neq I_C$.

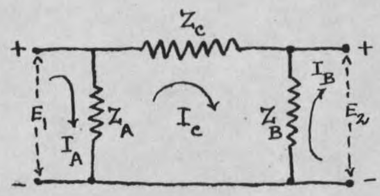

Fig. 2.

From Eq. 2

$$I_1 = \frac{1}{D}\,(d_{11}E_1 - d_{12}E_2) \quad \ldots\ldots \quad 6a.$$

$$I_2 = \frac{1}{D}\,(d_{12}E_1 - d_{22}E_2). \quad \ldots\ldots \quad 6b.$$

From Fig. 2

$$Z_A\,(I_A - I_C) = E_1$$

$$Z_B\,(I_B - I_C) = -E_2,$$

or,

$$I_A = E_1/Z_A + I_C \quad \ldots\ldots\ldots\ldots \quad 7a.$$

$$I_B = -E_2/Z_B + I_C\,. \quad \ldots\ldots\ldots\ldots \quad 7b.$$

From Eq. 6

$$I_1 - I_2 = \frac{1}{D}\left[(d_{11} - d_{12})E_1 - (d_{12} - d_{22})E_2\right].$$

From Eqs. 7

$$I_A - I_B = E_1/Z_A + E_2/Z_B\,.$$

Since $I_1 - I_2 = I_A - I_B$, these two equations give

$$Z_A = \frac{D}{d_{11} - d_{12}} \quad \ldots\ldots\ldots\ldots \quad 8a.$$

$$Z_B = \frac{D}{d_{22} - d_{12}}\,. \quad \ldots\ldots\ldots\ldots \quad 8b.$$

Again from Eqs. 7. $I_A + I_B = E_1/Z_A - E_2/Z_B + 2I_C$.

If in this equation values of I_A and I_B are substituted from Eqs. 6 and values of Z_A and Z_B from Eqs. 8, and since $I_1 = I_A$ and $I_2 = I_B$,

$$I_C = \frac{d_{12}}{D} E_1 - \frac{d_{12}}{D} E_2.$$

Applying Kirchhoff's law to the meshes of the circuit in Fig. 2,

$$(Z_A + Z_B + Z_C)\, I_C = Z_A I_A + Z_B I_B,$$

or,

$$(Z_A + Z_B + Z_C)\, I_C = E_1 - E_2 + (Z_A + Z_B)\, I_C,$$

which is obtained by substitution of Eqs. 7. Inserting the value of I_C from above and reducing,

$$Z_C = D/d_{12} \quad \text{.......} \quad 8c.$$

All equations 8 are perfectly general and applicable to any complex network.

If in Eqs. 8 the values of D and d's are substituted from Eqs. 5 and reduced,

$$Z_A = \frac{Z_1 Z_2 + Z_2 Z_3 + Z_1 Z_3}{Z_2} \quad \text{......} \quad 9a.$$

$$Z_B = \frac{Z_1 Z_2 + Z_2 Z_3 + Z_1 Z_3}{Z_1} \quad \text{......} \quad 9b.$$

$$Z_C = \frac{Z_4 (Z_1 Z_2 + Z_2 Z_3 + Z_1 Z_3)}{Z_1 Z_2 + Z_2 Z_3 + Z_1 Z_3 + Z_3 Z_4} \quad \text{......} \quad 9c.$$

1c. Expression for transmission.

From the equivalent Pi-circuit the expression for transmission may be derived as follows:-

From Eqs. 7

$$E_1 = Z_A\,(I_A - I_C)$$

$$E_2 = -Z_B\,(I_B - I_C).$$

Applying Kirchhoff's laws to the central mesh of Fig. 2,

$$Z_A\,(I_A - I_C) + Z_B\,(I_B - I_C) - Z_C I_C = 0.$$

Under no load conditions $I_2 = I_B = 0$. Hence the above equation reduces to

$$Z_A\,(I_A - I_C) - Z_B I_C - Z_C I_C = 0. \quad \ldots\ldots \quad 10a.$$

or,

$$\frac{I_C}{I_A - I_C} = \frac{Z_A}{Z_B + Z_C}. \quad \ldots\ldots \quad 10b.$$

Combining Eqs. 7 and 10b, the expression for T under no load conditions becomes

$$T = \frac{E_2}{E_1} = \frac{Z_B I_C}{Z_A(I_A - I_C)} = \frac{Z_B}{Z_A}\cdot\frac{Z_A}{Z_B + Z_C} = \frac{Z_B}{Z_B + Z_C},$$

or,

$$T = \frac{1}{1 + Z_C/Z_B}. \quad \ldots\ldots \quad 11.$$

If in this equation the values of Z_C and Z_B are inserted from Eqs. 9, the expression for T may be seen to be identical with Eq. 4.

Bridged-T Network Type 1.

2. General

The general mathematical theory developed above for any bridged-T network will be applied to the bridged-T circuit shown in Fig. 3. Comparing Fig. 3 with Fig. 1

$Z_1 = 1/j\omega C = -jX_c$, ———————14a

$Z_2 = k/j\omega C = -jkX_c$———————14b

$Z_3 = R$, ———————————14c

$Z_4 = R_s + j\omega L_s = R_s + jX_s$, -14d

where $\omega = 2\pi f$ = angular frequency.

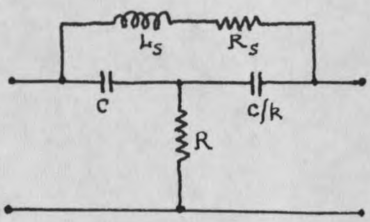

Fig. 3.

2a. Resonance.

Upon substituting the values of the component impedances from Eqs. 14 into the condition of resonance given by Eq. 5, and rearranging the terms, the condition of resonance for this circuit becomes

$$(-kX_c^2 + RR_s) + j\,(RX_s - RX_c - kRX_c) = 0.$$

For this equation to be true both the real and imaginary parts must vanish separately. Hence the two conditions of resonance for the circuit are

$$R.R_s = k.X_c^2\,, \qquad \text{or,} \qquad R.R_s = k/(\omega C)^2\,, \quad ....15.$$

and $$X_s = (1+k)\,X_c, \qquad \text{or,} \qquad \omega L_s = (1+k)/\omega C. \quad ...16.$$

2b. Transmission.

Substituting the values of the component impedances from Eq. 14 into the general expression for transmission given by Eq. 4,

$$T = \frac{1}{1 + \frac{-jX_c(R_s + jX_s)}{-kX_c^2 - jkRX_c - jRX_c + R\,(R_s + jX_s)}}$$

$$= \frac{1}{1 + A},$$

where $$A = \frac{X_cX_s - jR_sX_c}{(RR_s - kX_c^2) + jR\left[X_s - (1+k)X_c\right]}.$$

It may be noted, by substituting the resonant conditions in the above expression for T, that the circuit transmission is zero at resonance, as it should be. Let ω_o be the resonant angular frequency of the circuit, and let the inductive and capactive reactances at the resonant frequency be denoted by X_{so} and X_{co}, respectively. The conditions of resonance can therefore be written in the form

$$R.R_s = k.X_{co}^2 \quad \text{................15.}$$

$$X_{so} = (1+k)\,X_{co}\,. \quad \text{................16.}$$

Now if $\gamma = f/f_o$ and $Q_o = \omega_o L_s/R_s$,

the numerator of $A = \frac{X_{co}}{\gamma}\,\gamma X_{so} - j\,\frac{X_{so}}{Q_o}.\,\frac{X_{co}}{\gamma}$

$= X_{co}X_{so}\,(1 - j/\gamma Q_o)$,

and the denominator of $A = \left[kX_{co}^2 - kX_{co}^2/\gamma^2 + jR\left[\gamma X_{so} - (1+k)X_{co}/\gamma\right]\right.$

$R_sX_c = R_s\frac{1}{\omega C} = R_s\cdot\frac{1}{2\pi fC} = \frac{1}{\frac{1}{R_s}}\cdot\frac{f_o}{f(2\pi f_oC)} = \frac{f_o}{\frac{f}{R_s}}\cdot X_{co} = \frac{1}{\frac{f}{f_oR_s}}X_{co}$

$= \frac{R_s}{\gamma}X_{co} = \frac{X_{so}}{Q_o}\cdot\frac{X_{co}}{\gamma}$

$$= kX_{co}^2 (1 - 1/\gamma^2) + j \frac{kX_{co}^2}{R_S} \left[\gamma X_{so} - X_{so}/\gamma\right]$$

$$= kX_{co}^2 (1 - 1/\gamma^2) + jkX_{co}^2 . Q_o \gamma (1 - 1/\gamma^2).$$

$$\therefore \quad A = \frac{X_{so} (1 + 1/j\gamma Q_o)}{kX_{co}(1 - 1/\gamma^2)\ (1 - j\gamma Q_o)}$$

$$= \frac{X_{so}}{kX_{co}} . \frac{\gamma}{\gamma^2 - 1} . \frac{1}{jQ_o} . = j \frac{1 + k}{k} . \frac{\gamma}{1 - \gamma^2} . \frac{1}{Q_o} .$$

Hence,

$$T = \frac{1}{1 + j \dfrac{\gamma}{1 - \gamma^2} . \dfrac{1 + k}{k} . \dfrac{1}{Q_o}} \quad \ldots\ldots\ldots 17.$$

2c. Input and output impedances.

The component impedances of the equivalent Pi-circuit of Fig. 3 become, on substitution of Eqs. 14 into Eq. 9,

$$Z_A = \frac{kX_c^2 + j(1+k)\ RX_c}{jkX_c} \quad \ldots\ldots\ldots 20.$$

$$Z_B = \frac{kX_c^2 + j(1+k)\ RX_c}{jX_c} \quad \ldots\ldots\ldots 21.$$

$$Z_C = \frac{\left[R_S + jX_S\right]\left[kX_c^2 + j(1+k)\ RX_c\right]}{kX_c^2 + j(1+k)\ RX_c - R(R_S + jX_S)} . \quad \ldots\ldots\ldots 22.$$

It should be noted here that from these equations the value of T could be found.

The input impedance of the circuit at resonance is, from Eqations 12 and 20,

$$Z_{io} = Z_A = \frac{kX_{co}^2 + j\,(1+k)\,RX_{co}}{jkX_{co}}$$

$$= -jX_{co} + \frac{1+k}{k}\,R.$$

Since $Q_o = X_{so}/R_s$, it is evident from the resonant conditions that

$$X_{co} = \frac{1+k}{k} \cdot \frac{R}{Q_o}.$$

Therefore, $$Z_{io} = \frac{1+k}{k}\,R\,(1 - j/Q_o).$$

Hence, the magnitude of the input impedance at resonance is

$$|Z_{io}| = \frac{1+k}{k}\,R\sqrt{1 + 1/Q_o^2}\,. \qquad \ldots\ldots\ldots\ldots 23.$$

Similarly, the output impedance of the circuit at resonance is, from Eqs. 13 and 21,

$$(Z_{out})_o = Z_B = kZ_A.$$

$$\text{or,}\quad (Z_{out})_o = (1+k)\,R\,(1 - j/Q_o).$$

Hence, the magnitude of the output impedance at resonance is

$$|(Z_{out})_o| = (1+k)\,R\sqrt{1 + 1/Q_o^2}\,. \qquad \ldots\ldots\ldots 24.$$

Bridged-T Network Type 2.

3. General

The general mathematical theory will now be applied to the second type of bridged-T circuit which is shown by Fig. 5. Comparing Fig. 5 with Fig. 1,

$Z_1 = 1/j\omega C = -jX_c$ .. 25a

$Z_2 = k/j\omega C = -jkX_c$ .. 25b

$Z_3 = \dfrac{R_p \cdot j\omega L_p}{R_p + j\omega L_p} = \dfrac{R_p \cdot jX_p}{R_p + jX_p}$ .. 25c

$Z_4 = R.$ 25d

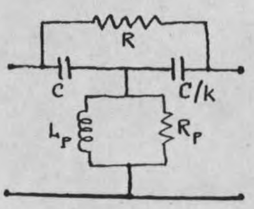

Fig. 5.

3a. Resonance.

Substituting the values of the component impedances from Eqs. 25 into the general condition of resonance given by Eq. 5, the condition of resonance for this circuit becomes

$$-kX_c^2 + \frac{kX_cR_pX_p}{R_p + jX_p} + \frac{X_cR_pX_p}{R_p + jX_p} + \frac{jRR_pX_p}{R_p + jX_p} = 0$$

or,
$$-kX_c^2 + \frac{kX_cR_p^2X_p + X_cR_p^2X_p + RR_pX_p^2}{R_p^2 + X_p^2} + j\frac{RR_p^2X_p - kX_cR_pX_p^2 - X_cR_pX_p^2}{R_p^2 + X_p^2} = 0.$$

For this condition to be satisfied, both the real and imaginary parts must vanish separately. Equating the real part to zero,

$$(1+k)\, X_c R_p^2 X_p + R R_p X_p^2 = k X_c^2\,(R_p^2 + X_p^2). \qquad \text{..........26.}$$

Equating the imaginary part to zero,

$$R.R_p = (1+k)\, X_c . X_p\ . \qquad \text{..........27.}$$

Inserting Eq. 27 in Eq. 26,

$$R.R_p(R_p^2 + X_p^2) = k X_c^2\,(R_p^2 + X_p^2),$$

and since $R_p^2 + X_p^2 \neq 0$,

$$R.R_p = k X_c^2\ . \qquad \text{..........28.}$$

Substituting Eq. 28 in Eq. 27,

$$X_p = \left[k/(1+k)\right] X_c\ . \qquad \text{..........29.}$$

Hence, the two conditions of resonance for the circuit are

$$R.\,R_p = k/(\omega C)^2 \ \text{..........................28.}$$

and

$$\omega\, L_p = k/(1+k)\omega C. \qquad \text{....................29.}$$

3b. Transmission.

Substituting the values of the component impedances from Eq. 25 into the general expression of transmission given by Eq. 4,

$$T = \cfrac{1}{1 + \cfrac{-jX_c R}{-kX_c^2 + \cfrac{X_p X_c R_p}{R_p^2 + X_p^2}(1+k)(R_p - jX_p) + j\,\cfrac{R_p . R X_p (R_p - jX_p)}{R_p^2 + X_p^2}}}$$

$$= \frac{1}{1 + A},$$

where,

$$A = \frac{jRX_c\,(R_p^2 + X_p^2)}{kX_c^2(R_p^2 + X_p^2) - R_pX_p\,(R_p - jX_p)\,\left[(1+k)\,X_c + jR\right]}.$$

If the inductive and capacitive reactances at the resonant frequency be denoted by X_{po} and X_{co}, respectively, the conditions of resonance may be put in the form

$$R.R_p = k.X_{co}^2 \qquad \ldots\ldots\ldots\ldots\ldots\ldots 28.$$

$$X_{po} = \left[k/(1+k)\right] X_{co}. \qquad \ldots\ldots\ldots\ldots\ldots\ldots 29.$$

If the ratio of the reactance of the coil and the resistance of R_p at the resonant frequency be denoted by Q_o i.e. if $Q_o = \omega_o L_p/R_p$,

$$\text{the numerator of } A = jRX_cR_p^2\,(1 + \gamma^2Q_o^2)$$

$$= jkX_{co}^2 . \frac{X_{co}}{\gamma} . \frac{X_{po}}{Q_o}\,(1 + \gamma^2Q_o^2)$$

$$= j\,\frac{X_{co}^2X_{po}}{\gamma Q_o}\,(1+k)X_{po}(1 + \gamma^2Q_o^2).$$

$$\text{the denominator of } A = kX_c^2(R_p^2+X_p^2) - (1+k)R_p^2X_pX_c - RR_pX_p^2 + j\left[(1+k)R_pX_cX_p^2 - RR_p^2X_p\right]$$

$$= \frac{kX_{co}^2}{\gamma^2}\,R_p^2(1+X_p^2/R_p^2) - (1+k)\frac{X_{po}^2}{Q_o^2}\,X_{po}X_{co} - kX_{co}^2\gamma^2X_{po}^2 + jR_pX_p\left[(1+k)X_cX_p - RR_p\right]$$

$$= \frac{kX_{co}^2}{\gamma^2} . \frac{X_{po}^2}{Q_o^2}\,(1+\gamma^2Q_o^2) - \frac{X_{po}^2}{Q_o^2}kX_{co}^2 - k\gamma^2X_{co}^2X_{po}^2 + jR_pX_p\left[(1+k)X_{co}X_{po} - RR_p\right].$$

Since the last term in the parenthesis is zero by Eqs. 28 and 29, the above is

$$= \frac{X_{co}^2X_{po}^2}{Q_o^2}\;k\,(1 + \gamma^2Q_o^2)(1 - \gamma^2)/\gamma^2.$$

ok

Therefore,

$$A = \frac{j\,\dfrac{1+k}{\gamma Q_o}\,X_{co}^2 X_{po}^2 (1+\gamma^2 Q_o^2)}{\dfrac{X_{co}^2 X_{po}^2}{Q_o^2}\,k\,(1+\gamma^2 Q_o^2)(1-\gamma^2)/\gamma^2}$$

$$= j\,\frac{1+k}{k}\cdot\frac{\gamma}{1-\gamma^2}\cdot Q_o.$$

Hence,

$$T = \frac{1}{1 + j\dfrac{\gamma}{1-\gamma^2}\cdot\dfrac{1+k}{k}\cdot Q_o}. \quad \text{..........30.}$$

3c. Input and output impedances.

Component impedances of the equivalent Pi-circuit of Fig. 5 become, upon substitution of Eq. 25 in Eq. 9,

$$Z_A = \frac{kX_c^2 - X_c X_p R_p\,(1+k)(R_p - jX_p)\;/\;(R_p^2 + X_p^2)}{jkX_c} \quad \text{........33.}$$

$$Z_B = \frac{kX_c^2 - X_c X_p R_p\,(1+k)(R_p - jX_p)\;/\;(R_p^2 + X_p^2)}{jX_c} \quad \text{.......34.}$$

$$Z_C = \frac{R\,[-kX_c^2 + X_c X_p R_p\,(1+k)(R_p - jX_p)\;/\;(R_p^2+X_p^2)]}{-kX_c^2 + X_c X_p R_p (1+k)(R_p - jX_p)/(R_p^2+X_p^2) + jRR_p X_p/(R_p+jX_p).} \quad \text{........35.}$$

It may be noted here that from these equations the value of T as given in Eq. 30 could be found.

The input impedance of the circuit at resonance is, from Eqs. 12 and 33,

$$Z_{io} = \frac{kX_{co}^2 - X_{co}X_{po}R_p\ (1+k)(R_p-jX_{po})/(R_p^2+X_{po}^2)}{jkX_{co}}$$

$$= \frac{kX_{co}(R_p^2+X_{po}^2) - (1+k)R_pX_{po}(R_p-jX_{po})}{jk(R_p^2+X_{po}^2)}$$

$$= \frac{(1+k)X_{po}(1+Q_o^2)-(1+k)X_{po}(1-jQ_o)}{jk(1+Q_o^2)}$$

$$= \frac{1+k}{k} \cdot \frac{X_{po}}{1+Q_o^2} \cdot Q_o(1-jQ_o)\ .$$

The magnitude of the input impedance at resonance is,

$$|Z_{io}| = \frac{1+k}{k} \cdot X_{po}Q_o/\sqrt{1+Q_o^2}$$

$$= \frac{1+k}{k} \cdot Xpo/\sqrt{1+1/Q_o^2}\ . \qquad \text{.................36.}$$

Similarly, the output impedance of the circuit at resonance is, from Eqs. 13 and 34,

$$(Z_{out})_o = Z_B = kZ_A.$$

$$\text{or,} \qquad (Z_{out})_o = (1+k)\frac{X_{po}Q_o}{1+Q_o^2} \cdot (1-jQ_o).$$

Hence, the magnitude of the output impedance at resonance is

$$(Z_{out})_o = (1+k)\ X_{po}/\sqrt{1+1/Q_o^2}\ . \qquad \text{.............37.}$$

4. Capacity Correction.

In the following analysis the actual resonant conditions and the effective capacity will be determined when the stray capacity c, between the junction point and ground is considered.

4a. Circuit 1. Comparison of Fig. 4 with Fig. 1 gives

$$Z_1 = -jX_c. \quad \text{———— 38a}$$

$$Z_2 = -jkX_c. \quad \text{———— 38b}$$

$$Z_3 = -jxR/(R-jx), \text{ (where } x = 1/\omega c.) \quad \text{———— 38c}$$

$$Z_4 = R_s + jX_s. \quad \text{———— 38d.}$$

Substituting Eqs. 38 in the general condition of resonance given by Eq. 5,

$$-kX_c^2 - \frac{jRx}{R - jx}\left(-jX_c - jkX_c + R_s + jX_s\right) = 0$$

or, $-kX_c^2(R^2 + x^2) + RR_s x^2 + R^2 x\left\{X_s - (1+k)X_c\right\} - j\left[R^2 x R_s - Rx^2\left\{X_s - (1+k)X_c\right\}\right] = 0.$

For this equality, both the real and imaginary parts must vanish.

Equating the imaginary part to zero,

$$R.R_s/x = X_s - (1+k)X_c. \quad \text{............39.}$$

Equating the real part to zero,

$$-kX_c^2(R^2/x^2 + 1) + RR_s + (R^2/x)\left\{X_s - (1+k)X_c\right\} = 0.$$

Since c is very small, $x^2 >> R^2$. Therefore,

$$-kX_c^2 + RR_s + (R^2/x)\left\{X_s - (1+k)X_c\right\} = 0.$$

Substituting Eq. 39 in this equation,

$$-kX_c^2 + RR_s(1 + R^2/x^2) = 0.$$

Neglecting R^2/x^2 compared with unity, the above equation reduces to

$$R.R_s = kX_c^2. \qquad \text{...............15.}$$

This resonant condition therefore remains, to a first approximation, unaffected by the stray capacity.

Inserting Eq. 15 into Eq. 39

$$X_s = X_c\,(1+k) + kX_c^2/x,$$

where the second term kX_c^2/x represents the correction term, which is negligible only when C is much larger than c. From the above equation,

$$X_s = X_c[\,(1+k) + kc/C\,]$$

or,

$$\omega L_s = [(1+k)/\omega C][1 + kc/(1+k)C] \quad . \quad \text{....40.}$$

Thus the resonant frequency is slightly increased by c. The effective circuit capacity in the presence of c is, from Eq. 40,

$$C' = \frac{C^2}{(1+k)\,C + kc}. \qquad \text{............41.}$$

where kc is the correction term. If c negligible

$$C' = C/(1+k).$$

as obtained earlier. For a symmetrical circuit, k = 1, and hence the effective capacity is

$$C' = C^2/(2C + c).$$

as obtained by Tuttle.

<u>4b. Circuit 2.</u> Comparison of Fig. 6 with Fig. 1 gives

$$Z_1 = -\,jX_c \quad \text{------------------42a}$$

$$Z_2 = -\,jkX_c \quad \text{------------------42b}$$

$$Z_3 = [R_p.jX_p.(-jx)]/[R_p.jX_p - R_p.jx + X_p x] \text{-42c}$$

$$Z_4 = R. \quad \text{------------------42d}$$

where $x = 1/\omega c$.

Substituting Eqs. 42 in the general condition of resonance given by Eq. 5,

$$-kX_c^2 + \frac{R_pX_px}{X_px + j(R_pX_p - R_px)}\left[R - j(1+k)\,X_c\right] = 0$$

or,
$$-kX_c^2x^2\left[X_p^2 + R_p^2\,(1-X_p/x)^2\right] + R_pX_px\left[RX_px - (1+k)R_pX_c(X_p - x)\right.$$
$$\left. - j\left\{RR_p(X_p - x) + (1+k)X_cX_px\right\}\right] = 0.$$

For this to be true both the real and imaginary parts must vanish.

Equating the imaginary part to zero,

$$RR_p(1-X_p/x) = (1+k)\,X_cX_p\,. \qquad \ldots\ldots\ldots\ldots 43.$$

Equating the real part to zero,

$$-kX_c^2x^2\left[X_p^2+R_p^2(1-X_p/x)^2\right] + R_pX_px^2\left[RX_p+(1+k)R_pX_c\,(1-X_p/x)\right] = 0.$$

Substituting from Eq. 43 and dividing by x^2,

$$-kX_c^2\left[X_p^2+R_p^2\,(1-X_p/x)^2\right] + RR_p\left[X_p^2+R_p^2\,(1-X_p/x)^2\right] = 0.$$

Since $X_p^2 + R_p^2\,(1-X_p/x)^2 \neq 0$, the above equation reduces to

$$R.R_p = kX_c^2\,. \qquad \ldots\ldots\ldots\ldots 28.$$

which is one of the conditions of resonance previously developed. Hence the stray shunting capacity has no effect on this condition.

Inserting Eq. 28 into Eq. 43

$$kX_c^2(1-X_p/x) = (1+k)\,X_cX_p$$

or,
$$X_p = kX_c/\left[(1+k) + kX_c/x\right]$$

or
$$\omega L_p = 1\,/\omega\left[(1+k)\,C/k + c\right]. \qquad \ldots\ldots\ldots\ldots 44.$$

where c represents the correction term and is negligible only when $c \ll C$. The new resonant conditions when c is not negligible are given by equations 28 and 44.

The effective circuit capacity in the presence of c is, from Eq. 44,

$$C' = (1+k)\ C/k + c. \qquad \text{.............45.}$$

If c is negligible,

$$C' = (1+k)\ C/k\ .$$

as obtained before. For a symmetrical circuit $k = 1$, and hence the effective capacity is,

$$C' = 2C + c\ .$$

as obtained by Tuttle. Here c is the correction term.

Equivalent Pi Circuit.

It may be mentioned here for interest that the equivalent Pi-circuit of the bridged-T networks, and consequently the whole mathematical theory of bridged-T networks, could also be derived from the very simple consideration given below. This was not used because the method which has been adopted in this thesis work for the development of the mathematical theory is a very powerful one that can be used on any complex network.

This simple method consists of first transforming the T section of the circuit into its equivalent Pi section, and then combining the bridging section with the series impedance of the Pi-circuit, as shown below.

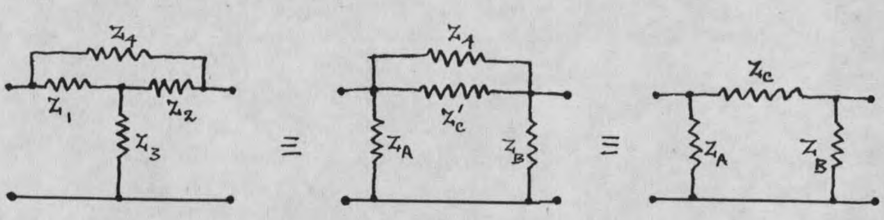

a b c

Fig. 20.

$$Z_A = (Z_1Z_2 + Z_2Z_3 + Z_1Z_3) / Z_2 .$$ [1]

$$Z_B = (Z_1Z_2 + Z_2Z_3 + Z_1Z_3) / Z_1 .$$

$$Z_C' = (Z_1Z_2 + Z_2Z_3 + Z_1Z_3) / Z_3 .$$

Again combining Z_4 with Z_C', the component impedances of the equivalent Pi-circuit are

$$Z_A = (Z_1Z_2 + Z_2Z_3 + Z_1Z_3) / Z_2$$

$$Z_B = (Z_1Z_2 + Z_2Z_3 + Z_1Z_3) / Z_1$$

$$Z_C = \frac{Z_C'Z_4}{Z_C' + Z_4} = \frac{Z_4\,(Z_1Z_2 + Z_2Z_3 + Z_1Z_3)}{Z_1Z_2 + Z_2Z_3 + Z_3Z_4 + Z_1Z_3}$$

which are exactly the equations obtained on page 69.

---

1. W.L.Everitt, COMMUNICATION ENGINEERING, Second edition, pp 38.